Corrosion inhibition of low carbon steel in soil solutions, using novel Schiff base inhibitors.

By

Mehmoona Faryal

School of Chemical and Materials Engineering

National University of Science and Technology

2021

Corrosion inhibition of low carbon steel in soil solutions, using novel Schiff base inhibitors.

Mehmoona Faryal

2018-MS-MSE-013-00000275068

This work is submitted as partial fulfillment of the requirements for the degree of

MS in Material and Surface Engineering

Supervisor: Prof. Dr Muhammad Shahid

School of Chemical and Materials Engineering (SCME)

National University of Sciences and Technology (NUST)

H-12 Islamabad, Pakistan

September, 2021

DEDICATIONS

To my compassionate late parents and

my supportive family.

ACKNOWLEDGEMENTS

It is my honour to show my most profound appreciation to my supervisor ***Prof. Dr Muhammad Shahid***, for his guidance and assistance throughout my experimental and research work. He constantly supported and appreciated me. I am grateful to him for providing me with a chance to work under his supervision. His compliant and thoughtful conduct facilitated me to comprehend my work; without his consistent support, this work would not have been plausible by any means.

I am also immensely grateful to the GCE committee**,** ***Dr Shoaib Butt*** and ***Dr Zeeshan Ali***, for their insightful comments and encouragement throughout MS research.

I want to pay my cordial gratitude to ***Dr Muhammad Arfan*** and ***Mr Muhammad Uzman*** for providing us with synthesized novel inhibitors.

I want to thank my family, sisters, aunty, uncle and particularly my parents for the open doors they provided and for showing me everything of those capacities constrained by my creative horizon, strengthening me, understanding me, and aiding me to accomplish my dreams. Their inspirations and relationship have constantly saved me.

Completing the dissertation needed effort and constant support, and I have several people to pay gratefulness for tolerating me for the past years. ***Samah Adeel, Dure Shahwar, Hira Adeel, Rabbia Naz, Iffat Ilyas, Naira Hamid*** *and* ***Mahnoor Fatima*** have been unwavering in their professional and personal support.

Mehmoona Faryal

ABSTRACT

The investigation of Corrosion inhibition behaviour of synthesized amino acid-based Schiff base inhibitors was carried out. Its adsorption in two types of (5%) soil solutions was studied at room temperature, using potentiodynamic polarization and gravimetric techniques. The inhibition efficiency obtained at the optimum inhibitor concentration (300ppm) was a maximum of 64% in acidic, ranging from 18.66% to 64.42%. Also, 70% maximum efficiency was recorded in the neutral electrolyte, whereas the range of 3.88% to 70.6%. Moreover, the carbon steel behaviour in 3.5% NaCl and 5, 10 and 15% soil solution were studied using the weight loss method for 1440 days and experimental data then combined with modelled data for obtaining failure predictions of structure based on an increment of concentration of soil in the electrolyte. Also, the effect of soil concentration was investigated using electrochemical studies and obtained Tafel plot, which has verified that increasing the concentration of soil in the electrolyte, makes electrolyte more corrosive. Electrochemical studies results illustrated that the inhibitors worked well in a less acidic environment in one of the soil solutions, which was relatively acidic than the other. Experimental data of potentiodynamic study also indicated that the inhibitors were more inclined to adsorb on the anodic sites of the carbon steel sample. Thus, the inhibitors can be categorized as anodic inhibitors due to suppressing more anodic reactions on the carbon steel sample.

Keywords: Corrosion inhibition, Schiff base, anodic-type, electrochemical methods

List of Figures

List of Tables

Table of Contents

Chapter 1

1. Introduction

Metal is an essential raw material in any industry and development sector; thus, its importance for human civilization is inevitable [1]. Almost all metals are reactive and susceptible to deterioration in the environment because of the well-established phenomena of corrosion. Deterioration caused by the corrosion in industrial metallic alloys is due to the chemical interaction of the metals with the environment, which then requires maintenance and repair of the damage incurred [2]. Consequently, causing a good portion of industry loss can only be minimized by applying corrosion mitigating, controlling, and monitoring techniques. Although metals have numerous industrial applications, one of their primary uses is the transportation of fluids. Pipelines carry various fluids and are likely to develop corrosion inside the pipe wall [3].

To produce the extended structure of the pipe system, the most common metal used is carbon steel because of its effectiveness and availability as an economical metal despite that the fact corrosion resistance of carbon steel is relatively low [4], [5]; alternate metals with good corrosion resistance are costly. Thus, most industries prefer to rely on corrosion control and monitoring techniques to protect the metallic structures [6] from enhancing their service life for obvious reasons. Corrosion inhibitors may be considered an essential chemical addition to protecting carbon steels, among several corrosion control methods; the addition of a small concentration of inhibitors can minimize corrosion rate. Nevertheless, there is proviso facilitating selecting an inhibitor suitable for the specific situation [7]. The conditions include the stability and availability in the environment, the ability to protect and treat the surface being corroded, long-run toxicologic impacts on the environment, cost, and the inhibitors required for the specific situation [8, 9].

Adding corrosion inhibitors in the environment inside a pipe and protects the pipelines internally from corrosion. It decreases the attack rate of corrosion due to specific chemical compounds/species [10]. The renowned corrosion inhibitors are primarily based on organic compounds that contain oxygen, nitrogen, or sulphur atoms [11].

Organic inhibitors treat the surface of the metal and minimize corrosion by adsorption. In contrast, the Influence of this phenomenon is the function of electrolyte's aggressivity, inhibitor's chemical nature, surface charge, and nature of the metal [12].

Various natural and synthetic products are known to protect the surface of metals and alloys. Organic materials synthesized in the laboratory gain attention in industry after testing their inhibition activity [13, 14]. Schiff bases are organic compounds synthesized by Hugo Schiff, also recognized as imine or azomethine, basically like aldehyde or ketones. Only the carbonyl group is simply substituted by either imine or azomethine group. The presence of double bond and heteroatom play a crucial role in inhibition [15]. Also, the unique bond between electronegative nitrogen and hydrogen, whose electronegativity is low, makes this moiety polar. It provides more protection than the amine and aldehyde from which it is synthesized. The synthesized Schiff bases are made from cheap and environmentally friendly chemicals. Inhibition actions start when a metal loses electrons and then delocalizes; pi-electron makes strong coordination with metal and stops metal oxidation [16].

1.1. Adsorption mechanism of organic inhibitors

The organic inhibitors are adsorbing on the solution/metal interface by following a mechanism that completes one or more steps. In the first step, one or more water molecules replace initially absorbed species on the metal surface, thus facilitating the adsorption of organic inhibitors on the metal surface [17].

$$Inh_{Soln} + xH_2O_{Ads} Inh_{Ads} + H_2O_{Soln} \quad (1)$$

In the above equation, Inh_{Ads} and Inh_{Soln} denote the adsorbed inhibitors and the inhibitor present in the solution, respectively, whereas 'X represents the count of the molecules of water replaced by the molecules of inhibitor. As a result, the combination of a newly produced metal ion M^{+2} and inhibitor will occur on the surface of the metal because of the process of dissolution or the oxidation of metal, which creates the metal-inhibitor complex:

$$M \rightarrow M^{+2} + 2e^{-} \quad (2)$$

$$M^{+2} + Inh_{ads} \rightarrow [M - Inh]_{ads} + 2] \quad (3)$$

Further inhibition of metal dissolution is dependent on the resulting complex's relative solubility. The aggressive solution in the absence of corrosion inhibitor is continuously causing the metal dissolution as it remains in contact with the metal and causes the increment of corrosion by making a porous film on the surface. However, the role played by the inhibitor in solution is blocking the open or active sites in the porous surface with the assistance of adsorption of inhibitors, which construct the barrier layer and restrict the further reaction of corrosion [18].

1.2. Schiff bases corrosion inhibitors

Synthesis of Schiff bases is economical as the starting material is inexpensive, less perilous, and eco-friendly [19, 20]. Hence these inhibitors are getting popular for corrosion protection. Schiff bases inhibitors have proved to be more efficient for inhibiting corrosion than the contemporary aldehydes and amines inhibitors. These inhibitors perform efficiently due to the substitution of the π-electrons and the number of heteroatoms (e.g., Cl, Br, O, and N) in the structure and the functional group (C=N-) [21]. Subsequently, these molecules create a constantly adsorbed thin film, which slows down the cathodic, anodic, or sometimes both and minimize the corrosion rate (CR). As the inhibitors work through the process of adsorption on the solution/metal interface; thus, the inhibitor's efficiency depends upon the corrosive environment, the metal surface nature, and the presence of electrochemical potential on the surface of the metal [22-24]. Moreover, the inhibitor's structure, which involves the charge densities and the count of active centres for adsorption, the adsorption mode, molecule size, and the metal surface, the shielded area of inhibitor impacts the inhibitor's efficiency. Hence, it is essential to clarify the interaction between metal surfaces and inhibitor molecules to know the efficient and new corrosion inhibitors [21].

Using gravimetric and electrochemical techniques, this research will examine the inhibitory impact of various alcohol-soluble Schiff base compounds on carbon-steel corrosion in soil solutions made from two soil samples obtained from two different

locations. The findings of the experiments were combined with a theoretical technique and analysed.

Chapter 2

2. Literature Review

2.1. Corrosion Control Techniques

The mitigating corrosion strategies are used to control the corrosion to protect pipelines from failures and take preventive measures to secure pipelines that could lead to a range of dangerous situations such as environmental pollution, losses of products and accidents[25],[26]. There are five corrosion control mechanisms: selecting materials, design, the protective covering, chemical processing, and cathode protection. The above mechanisms are vital for the construction and design of pipelines, minimizing corrosion attacks [27].

2.2. Material Selection

Material selection is a prominent aspect of the designing of the pipeline system in order to mitigate corrosion. The material behaviour and mechanical properties in a particular environment are considerable components in material selection. The conservational condition can be named the pressure, velocity fluid chemistry, temperature, and water composition. Moreover, the material analysis, while selecting its compatibility as union connector, flanged connection, and fitting are compulsory; therefore, the galvanized corrosion can be resisted. [28]

However, carbon steel is the preferable choice in manufacturing pipelines for transportation of oil and gas because of its low cost, availability, and excellent mechanical properties. Regardless of low corrosion resistance quality as compared to the alloys that can resist corrosion well. Nevertheless, the higher corrosion rate is predicted the alloy with excellent corrosion resistance lining with carbon steel is a more practical choice as a material. [29]

2.3. Design

They design the corrosion control pipeline system, which plays an indispensable role in extending the life of the steel pipeline. Threaded joints, sharp edges, steel geometry, pipeline fitting and the welded joints are the most vulnerable locations for the localized

corrosion. As the fluid typically settles and penetrate at these spots. Moreover, these locations are easily attacked by corrosion because they are mostly poorly coated. Thus, the design factor should be carefully considered in order to limit corrosion. [30]

2.4. Protective Coating

NACE RP-01-69 covers the function and desired properties of a dielectric pipeline-type coating area. This specification aims to control corrosion through the isolation of the external surface of the underfloor or submerged pipe from the environment, reduce requirements for cathode protection, and improve the current protective distribution. Coatings shall be selected and applied appropriately, and a coated tube shall be carefully installed to perform these functions. Various coating types can perform the desired functions.[31] Efficient electrical insulation and moisture barriers, excellent adhesion, resistance to corrosion and constant electrical resistant over time, resistance to chemical degradation and rewinding, ease of reparation and retention of physical properties are the desired properties of the coating[32].

2.5. Chemical Treatment

The chemical treatment is beneficial to protect the pipeline from internal corrosion. For that purpose, the corrosion inhibitor is used. The corrosion inhibitors are injected into the pipeline either in slug treatment, continuous injection, or batching forms. The internal corrosion is resisted by the passive layer formed by the injected corrosion inhibitors that prevent the pipeline from direct contact with water or the fluid that is being transported through the pipeline [33].

2.6. Cathodic Protection

Cathodic protection functions by preventing the cathodic surface from occurring anodic reactions, and cathodic surfaces are essentially the structure under protection. The anodic reactions that supposedly occur on the structure; the CP system allows those reactions to occur on the specially designed and installed anode to protect the structures[34],[35]. Moreover, it can also be defined as the corrosion control electrochemical mean that suppresses the corrosion of on cathode of the galvanic cell and allows the oxidation reactions on the surface of the anode [36].

2.7. Electrochemical Analysis of Corrosion

2.7.1. Definition of Corrosion

The phenomena of corrosion appear on the metallic structures' surfaces, in which the electrochemical reaction initiated due to the presence of the corrosive environment serving as an electrolyte and the difference in the potential—this difference force electron from the anodic site toward the cathodic site passing through the electrolyte based medium. [37]

These electrochemical reactions, reduction, and oxidation give rise to the mechanical damages to the metal structure where oxidation reaction is happening and assist in producing rust, consequences of the reduction reactions. [38]

2.7.2. Parameters of Corrosion

The circuit of corrosion cell consists of specific factors that are compulsory to proceed with the corrosion phenomena, which include an electrolyte, cathode, electrical contact, and anode.

Anode

The metallic site in which metallic surfaces are oxidized is dissolved, and ions and electrons are produced. The electron leaves the anodic site by electric connection and enters the cathode site; ions vacate the metal surface and reach the electrolyte. The following reaction shows Fe (Iron) oxidation:

$$Fe \rightarrow Fe2+ + 2e- \qquad (4)$$

Several factors encourage anodic reactions, including electrolyte acidity, salt, and lower pH values, and oxidizes atoms in the iron surface by electricity loss from the cathodic site. Iron conductivity allows the reaction of oxidation to take place as an Eq.4.

Thus, the problem arises as to why electron travels from anodic to cathode sites. This response is a difference in the potential between the two sites, which results in an iron oxidation reaction. With the increment of the potential, water molecules encouraged the electrolyte to dissolve, as stated in the next equation. The Eq.5 indicates the oxidation reaction at the electrolyte/anode interface. [39]

$$2H_2O \rightarrow 4H + + O_2 + 4e^- \quad (5)$$

Cathode

The cathodic surface that is metal is the site where reduction reaction happens by consuming incoming electrons from the anodic site through the electrical correspondence. The electrolyte surrounding the cathode contains the hydrogen and oxygen ions, and by gaining electrons, the reduction reactions prevail. The reactions given represents the reduction of oxygen and hydrogen

$$2H + + 2e - \rightarrow H_2 \quad (6)$$

$$2O_2{}^- + 4e - \rightarrow O_2 \quad (7)$$

The hydroxide is a product of reducing water and oxygen with the combination of electrons released from the oxidation reaction. The following reaction shows the reduction reaction happening on the interface of the electrolyte/cathode [40].

$$O_2 + 2H_2O + 4e^- \rightarrow 4OH^- \quad (8)$$

Electrolyte

The electrolyte can be defined as the medium that promotes ions commuting from anode to cathode or vice versa; as the solution can conduct electricity, it can be entitled the corrosive solution. Because the dissolved positive and negative ions movement tends to make changes in the electrolyte part of the corrosive process, these changes are called electrolysis. The electrolyte can be any environment that conducts electricity, for instance, water, soil, or any other solution that tends to corrode metals [41].

2.7.3. Soil

The soil analysis is based on the element's inquiry present in the soil, which is water-soluble under the conditions and standards. The determination of the constituents is centered on two types of elements, which can be categorized as acid-forming and base forming. The acid-forming elements include chlorides, nitrates, carbonate, bicarbonates, and sulfate. At the same time, base-forming elements are magnesium, potassium,

calcium, and sodium. The ability, electricity conduction of soil can be determined by the moisture content of the soil combining the amount and the nature of the soluble salts [41].

To investigate the corrosion potential of the soil, the ascertainment of the moisture content in the soil is a crucial variable. Hence, the dry environments do not conduct electricity. Thus, zero to no corrosion is reported in such environments; thus, the resistivity of the soil in a dry environment is very high. Therefore, the increment of the moisture content in the soil tends to decrease the resistivity swiftly until the point of saturation arrives. After reaching a saturation point, the inclusion of moisture content has almost nil effect on the soil resistivity [42].

2.7.4. Effect of pH Value

As the abbreviation pH stands for the potential of hydrogen, it is principally used to gauge the hydrogen ions' concentration in the solution or substance. However, it is used to measure the acidity or basicity by utilizing the scale from 0 to 14 and 7 considered neutral. The pH greater than seven is considered the base, and the pH smaller than seven is considered acidic. A substance that consists of more hydrogen ions is considered acidic, whereas the solution containing more hydroxyl ions are known as the essential solution. The chemicals or constituents present in the solution determines the pH value. Therefore, it is considered a vital indicator of chemical changes. Each number present in the range represents 10-fold changes in the basicness/acidity of the solution, which means that six pH is ten times less acidic than five pH [43].

The pH value also evaluates the solubility of specific components in the substance; for instance, it can determine the abundance of phosphorus in the water. Lower pH value at which the affluence inclines to become more acidic enhances the chances of corrosion of metallic structures by supplicating hydrogen ions in abundance [44, 45].

External path: The electronic path or the obvious path is the must factor between the cathode and anode, through which electrons can commute during the oxidation process from anode to the cathode during the process of corrosion. Several theories have been explained in the electronic movement method as they move through the metals. According to one theory, as one of the outer-shell electron losses from an atom, it

collides with the atom's outer-shell next to it; this newcomer electron replaces the electron and makes it collide with the nearby outer-shell atom. This process continues until it approaches the surface of the cathode, where the reduction process consumes it [46].

As one of the electrons is produced at the anode, it must be gained on the cathode surface simultaneously. Hence, the process of reduction and oxidation reaction is happening equally. These electrons can only move in this obvious path but not in the electrolyte. Disrupting this process effectively, the corrosion rate, if the flow of electron is restricted somehow, then the corrosion process decelerates [31, 47].

Electrochemical corrosion cell: Four factors complete the corrosion cell, all the four items mentioned in the previous topics. These four items are a must for corrosion phenomena to occur. The free electrons would always opt for the obvious or electronic path to commute between the anode and cathode and never choose electrolytes. However, the ionic movement would always happen in the electrolyte medium, and practically the electrolyte for pipelines is soil or water environment. The ionic movement barriers in soil cases are the dry environment. Thus, anode and cathode can be present in variant electrolytes but must be present in the same electrolytic environment [48, 49].

2.8. Reference Electrode

Reference cells are used to measure the potential value between the metals by comparing the reference cells and the metal potential. The reference cell is based on the amalgamation of the solution consist of absolute ionic concentration and the metal electrode. This combination can gauge the potential of the immersed metal by acting as the stable half of the cell.

2.8.1. Copper Sulfate

One of the most popular reference electrodes in the corrosion control of the pipeline, known as ($Cu/CuSO_2$). Cathodic protection criteria are determined using $Cu/CuSO_2$ and are typically utilized in freshwater and soil environments. Moreover, in some instances, the Copper Sulfate reference electrode needs to be verified when contamination is

suspected or use of it is extended. This can be quickly done by comparing its potential with the newly charged Copper sulfate electrode. If the reported potential differs exceeding 10mV, then the cell under verification needs to be recharged or cleaned [49].

2.8.2. Silver-silver chloride

The chloride-based environment is considered corrosive, which the Copper Sulfate reference cannot withstand; thus, silver-silver chloride is used in such an environment. This electrode comes in two forms one is dry, and the other one is saturated. In the saturated one, potassium chloride is used as an electrolyte. Whereas, in the dry cell, the seawater is used in which the dry electrode is immersed. The presence of the chloride content varies the potential reading [50].

2.8.3. Other Reference electrodes

The mercury-based reference electrode is known as Calomel; it is only used in laboratories. Mercury electrodes are used in different concentrations of KCl, under the specific concentration of ions of mercury. Another type is hydrogen reference, which is considered delicate and cannot be used for fieldwork. Moreover, several other kinds of metals have been used; however, they are only useable in the laboratory environment [51].

2.9. Corrosion affecting Underground Pipeline

Many forms of corrosion can affect the underground pipeline due to the structure being based on metal, iron. The most common types of corrosion would be discussed in this section of the chapter. However, most of them can be controlled using coating, cathodic protection, and other forms of corrosion control. Corrosion protection methods can be failed, and corrosion can become a problem at any instant, and such type of corrosion may lead to pitting or several other localized corrosions.

The design of cathodic protection of the underground pipeline structure is the main aim of the study. Thus, it is vital to know the types of corrosion that can assist in protecting the pipelines using a Cathodic protection system [52].

2.9.1. Uniform Corrosion

The most commonly occurring type of corrosion is categorized as the steady loss of metal from the surface. This type of corrosion appears on the unprotected pipeline, never coated, or applied CP on it. In this kind of corrosion, there might be certain spots that experience pitting corrosion and more metal loss compared to other areas. However, overall, the loss of the metal from the surface is uniform in this case of corrosion [53, 54].

2.9.2. Pitting Corrosion

The type of corrosion is localized corrosion in which the holes are formed in the metallic structure. Uniform corrosion is less dangerous than pitting because it is more challenging to point out this kind of corrosion and thus become a hindrance in deigning. The pits are most of the time covered by the product forms because of corrosion. The small pits lose very few amounts of metal and thus can fail the whole structure [55].

2.9.3. Galvanised corrosion

The type of corrosion occurs when two metals having different potentials are somehow in contact while electrolyte is present. Because of this combination, one of the metals in contact, which is mainly at a lower potential than the other, becomes the prey of corrosion and consequently deteriorate [56].

2.9.4. Microbiologically influenced corrosion

Some microbial activities catalyse these reactions leading to corrosion, especially when the affected surface is in close contact with the organisms—reduction in the aerobic conditions caused by cathodic reactions. At the same time, the evolution of hydrogen plays the role of cathodic reaction in anaerobic conditions. These organisms tend to make a biofilm on the surface of the metal. The resultant deterioration of metal, known as microbially influenced corrosion (MIC) or biocorrosion [57].

2.10. Schiff Base Inhibitors

2.10.1. Methods of synthesis

Three general ways to synthesize Schiff base are as follows [58]:

1. Way 1: (Microwave Oven)

2. Way 2: (Reflux)
3. Way 3: (Stirring)

2.10.2. Schiff base used as a ligand to synthesize metal complexes for DNA binding studies

Mohammad Shakir et al. reported a Schiff base, synthesized by condensing 2-thiophene carboxaldehyde and 3,3'-diaminobenzidine. Ligand produced was then used to synthesize metal complexes with cobalt, nickel, copper, cadmium, and mercury. Both products were used in DNA binding studies. Different characterization techniques confirmed all products. Research revealed that complexes have more potential toward DNA than Schiff base. Among complexes, the copper shows best results. Crystal structure of ligand also reported in Figure-2.1 [59].

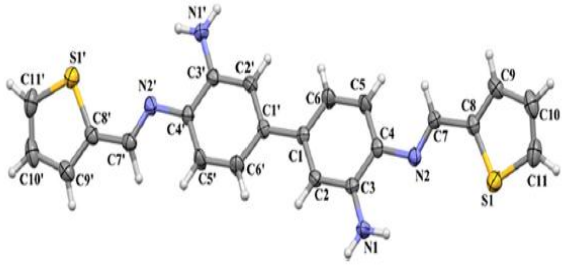

Figure 2.1: Structure of Schiff base ligand

2.10.3. Corrosion Inhibition

Schiff bases have the potential to protect the surface of the material from corrosion. Inhibition rate of 5-((E)-4-phenylbuta-1,3-dienylideneamino)-1,3,4-thiadiazole-2-thiol Schiff base were reported. Schiff base was synthesized by the reported method, and its inhibition potential was studied in 0.5M HCl. Characterization techniques utilized include potentio-dynamic polarization, EIS, linear polarization resistance, hydrogen gas evolution, the change of open circuit potential as a function of immersion time, SEM Figure-2.2 and AFM. Mechanism of inhibition includes covering active sites on the metal surface by Schiff base, specially heteroatoms present in its structure [60].

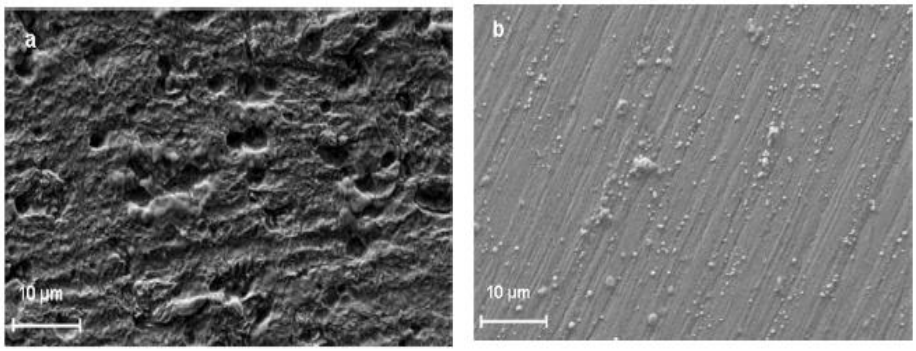

(a) (b)

Figure 2.2: SEM images of metal surfaces (a) without inhibitor (b) with inhibitor

Chapter 3

3. Methodology

3.1. Chemical composition of carbon steel alloy

The AISI 1040 carbon steel was used as a working electrode for which a surface area of 1 cm^2 was employed. The nominal properties of this steel are given in Table-1.

Table 3-1: Nominal properties of the carbon steel used.

Yield Strength	UTS	Elongation	Chemical composition
415 MPa	620 MPa	18%	C: 0.37-0.44 Mn: 0.6-0.9 S: ≤0.05 Fe: 98.6-99

3.2. Test solution

Two solutions were prepared with 5% soil concentration; soils were obtained from two locations: (1) NUST Islamabad, Pakistan, denoted by 'SCME soil solution' and (2) Wah, Pakistan, denoted by 'Wah soil solution.' These solutions were prepared by the 1:1 soil-to-water method, where 200 g of soil was put into the 500 ml beaker, and then 200 ml of distilled water was added; the solution was stirred for 20 minutes [61]. The filtered extract was placed on the hot plate and left for drying to obtain concentrated soil salt solution, then used to make the 5% solution of soil using distilled water. 300-ppm concentration was used for corrosion investigation; organic inhibitors were soluble in methanol and ethanol.

3.3. Measurement of Corrosivity

3.3.1. pH measurements

The pH of the soil was measured by making a soil solution in water with a ratio of 1:2, using a digital pH meter PCE-PH 26F; it was calibrated using pH 4,7 and 10 buffer solutions before use.

3.3.2. Ionic Conductivity

The ionic conductivity was determined using digital meter Jenway ® 4510; micro siemens recorded the measurements.

3.3.3. Total dissolved solids

Determination of total dissolved solid was performed using a digital setup Jenway ® 4510, and the TDS were recorded in milligrams per litre for each soil solution.

3.4. Soil Resistivity Measurements

3.4.1. Experimental Site

The site near SCME was selected; it was divided into three fields to confirm the soil resistivity of the area where the pipeline supposedly should have been buried. The test was performed in total 120 feet length of the site, as shown in Figure-3.1, whereas soil resistivity tests were performed in the three 60 feet selected areas of the total field.

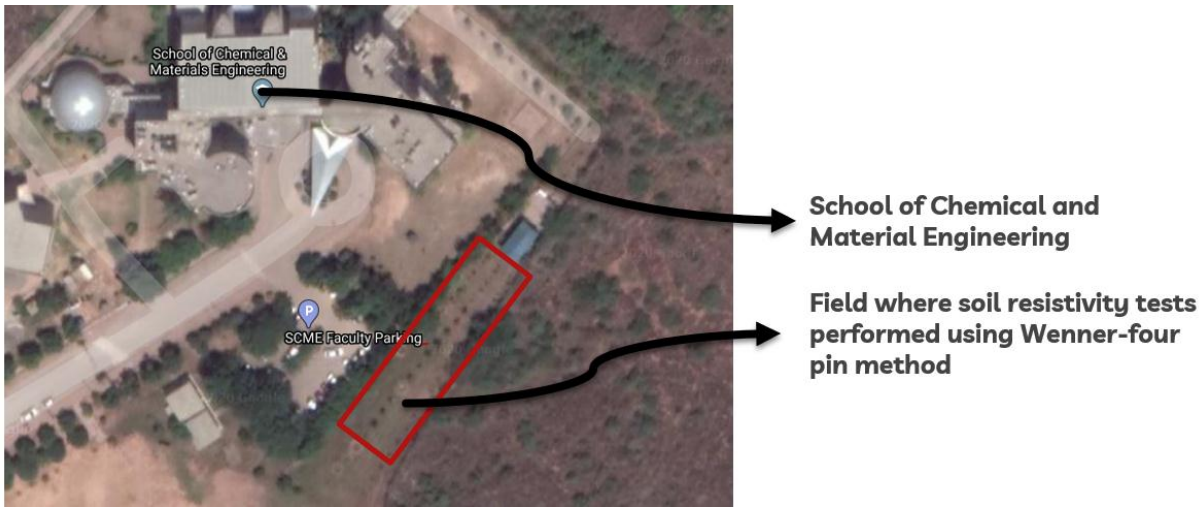

Figure 3.1: Experimental Site for Soil Resistivity Test

Figure-3.2 illustrates the chosen field for three different soil resistivity tests, which has confirmed soil resistivity, also due to which the soil corrosivity was confirmed.

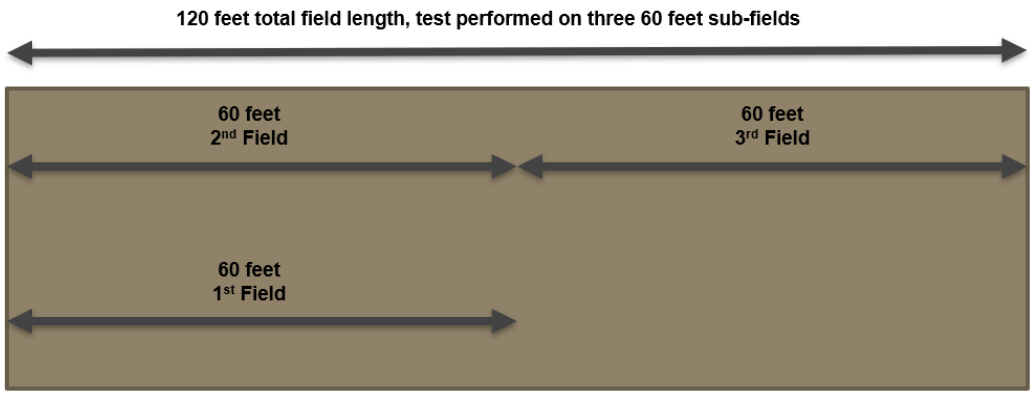

Figure 3.2: Three soil resistivity tests' field illustration

3.4.2. Wenner Four Pin Method

Several methods measure soil resistivity, but the Wenner Four pin method is the most popular among other measuring methods like Schlumberger. Electrical resistivity is expressed in ohmmeters; it measures the specific resistance of the material. Soil resistivity is also measured in ohmmeters and usually executed on the land sites while designing underground systems. The earth resistivity meter of model 'Super sting R1 IP' was used to measure the soil resistivity data. This equipment measures and calculates the soil resistivity data, automatically only setting was automatically required, which is illustrated in Figure-3.3.

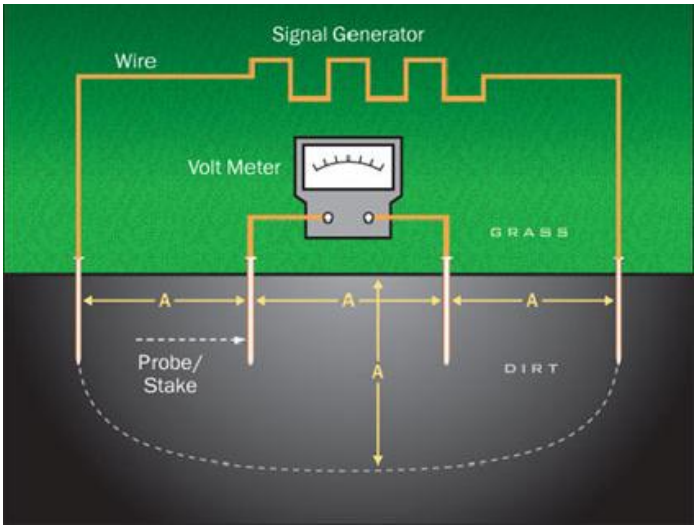

Figure 3.3: Wenner Four-pin Method [62]

Figure-3.3 shows the setting of the Wenner four-pole method and the connection of the wires in the setup. Four steel probes were used and inserted in the ground on equidistant locations vertically in the experimental setup. The depth was 1.5 feet, and 'A', the horizontal distance, was considered 5 feet, 10 feet and 15 feet. [62]

3.5. Corrosion measurements

The cylindrically mounted electrode of area (exposed surface area = 1 cm^2) was used for corrosion investigation. The potential (V) values were taken with reference Ag|AgCl| reference electrode. Before initiation of the experimental setup, soil solutions were prepared following the test solution recipe, whereas each experiment was performed thrice for consistency. To remove the contamination on the surface due to oxides, the working electrodes were stabilized at -1000 mV for five minutes in the solution; the solution was shaken so that the adsorbed hydrogen bubbles could be liberated. Then, the polarization experimentation was performed. Gamry® G750 electrochemical framework was used for all corrosion investigations.

3.5.1. Potentiodynamic measurements

The corrosion rate was determined by obtaining Tafel plots, where the current density was measured in the 5% soil solution with and without (300 ppm) Schiff base inhibitors/soil solutions. Cathodic and anodic Tafel slopes extrapolations were performed at ±250 mV potential range with reference to E_{corr}, at a scan rate of 1mV/s.

3.5.2. Linear polarization resistance CR

The corrosion rate was evaluated using the linear polarization resistance (LPR). The R_p of steel working electrode was measured in the 5% soil solution and (300 ppm) Schiff base soil/inhibitors solutions. The Gamry framework program did the variation of the working electrode through a Reference 600 potentiostat. The Gamry framework program converts corrosion current from nano ampere per square centimetre to a mills per year Corrosion rate. The working electrode of grade AISI 1040 of carbon steel was used, at ±20 mV, the small sweep is performed.

3.5.3. Weight loss measurements

The corrosion rate is investigated using weight loss measurements by experimentation and then calculating empirically, using the equation formulated by Ali, N. et al. [63]. The dimensions of the carbon steel specimen were 4 cm×1.5 cm×0.5 cm. First, these electrodes were polished using emery paper of grade 50 and then rinsed thoroughly using de-ionized water before immersing specimens into the solution. Weight loss is determined after every 20 days for two consecutive months of immersion in the 80cm^3 5% soil solution and 3.5% NaCl environment evaluate the corrosion rate in mills per year. Measurements were conducted at room temperature.

$$SA = [2(LH + BH + BL)] \tag{9}$$

Where SA is the surface area of the carbon steel specimen, B indicates the breadth of the sample, L is the length, and H is the height of the specimen [64].

The weight loss variation occurred by immersing the carbon steel specimen in the 3.5% NaCl solution and 5% soil solution for the span of 480, 960 and 1440 hours; a total of six specimens were prepared to conduct this experiment. The weight loss was measured taken following the ASTM standard G31-72 [65]. After performing the experiment, providing empirical modelling was essential because it can predict the theoretical weight loss. Weight change of low carbon steel specimen was plotted against the time of immersion, which provided the theoretical prediction of the weight change of the carbon steel. The predicted weight change of the carbon steel specimen assisted in calculating the corrosion rate using the quantitative analytical method. The corrosion rate (CR) can be calculated using the given equation[66]:

$$C_R = \frac{87.6(W_{L)}}{(SA)(t)(\rho)} \tag{10}$$

Where W_L is the weight loss of the specimen after specific immersion time *t, SA* is the surface area of the carbon steel sample, and ρ is the density of carbon steel. The empirical model for the theoretical prediction of corrosion rate was developed by plotting corrosion rate values of quantitatively collected data against the concentration of the NaCl and the soil solution.

Chapter 4

4. Results and Discussion

4.1. Measurement of Corrosivity

Investigations were carried out and presented to determine the corrosivity measurement of soil, pH, Ionic conductivity, and total dissolved solids.

4.1.1. pH Measurement

Several studies reported on the buried metallic structure and their corrosion suggested that the pH values of soil matter and the structures are susceptible to corrosion at any given pH value. However, it dominates when the range pH value exceeds the range of 4 to 8.5. However, acidic soil has higher risks of deterioration of structure structures due to corrosion[67]. In contrast, alkaline soil tends to develop deposits on the surfaces due to the high calcium and magnesium concentrations, which sometimes protect the surfaces from corrosion attacks—the popular methods of measuring pH using colour altering pH papers and measuring through the digital pH meter. In the present study pH of the soil is investigated using the digital pH meter [68].

The soil solutions' pH and solutions containing inhibitor were in between the range of those soil samples come under 6.75-7.55 as shown in Table-4.1. Therefore, Figure-4.1 can be considered neutral as the environment under the range of pH from 6-8 [69]. Whereas some of the inhibitor-based soil solutions are inclined toward the acidic values of pH, the inhibitor's behaviour shows that the minorly acidic environment is created by the inhibitor's behaviour show in the soil solution.

Table 4.1: pH of the 5%soil solutions with and without Schiff base inhibitor; 'SCME and Wah soils.'

Inhibitor based 5% soil solution	SCME soln. pH	WAH soln. pH
AB24	6.75	7.15
AB36	6.77	6.85
AB22	6.79	7.18
AB33	6.79	7.42
AB34	6.94	7.20
AB41	6.74	6.9
AB55	6.81	7.05
AB59	6.90	7.06
AB19	7.10	7.17
5% Soil Solution	**7.55**	**7.56**

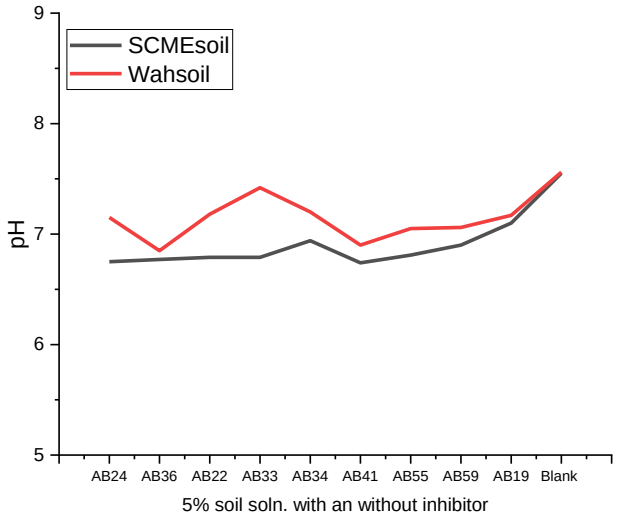

Figure 4.1: pH of two types of 5% soil solution, SCME and Wah with and without Schiff base inhibitors

4.1.2. Ionic Conductivity Measurement

Ionic conductivity measurement reports the presence of Ions in the electrolyte that enables the solution to conduct electricity. The Ionic conductivity of the solution increases as the salts are present; likewise, if the soil is saline, the ionic conductivity of its solution would be higher. In the current study, the Ionic conductivity ranges from 72 – 325 µS. According to the manual, [70] the corrosive water-based electrolyte should be

more than >100µS. The results indicate that the 5% soil solution can create the corrosive media for the steel pipeline carrying water inside [71].

Table 4.2: Ionic Conductivity Measurement of SCME and Wah soil soln. in the presence and absence of Schiff base inhibitors

Inhibitor based 5% soil soln.	SCME soln. IC (µS)	WAH soln. IC (µS)
AB24	216	102.8
AB36	155.8	112.9
AB22	164.1	135.9
AB33	152.5	75
AB34	160	244
AB41	161.1	296
AB55	176.9	259
AB59	147	325
AB19	100	200
5% Soil Solution	**262**	**154.7**

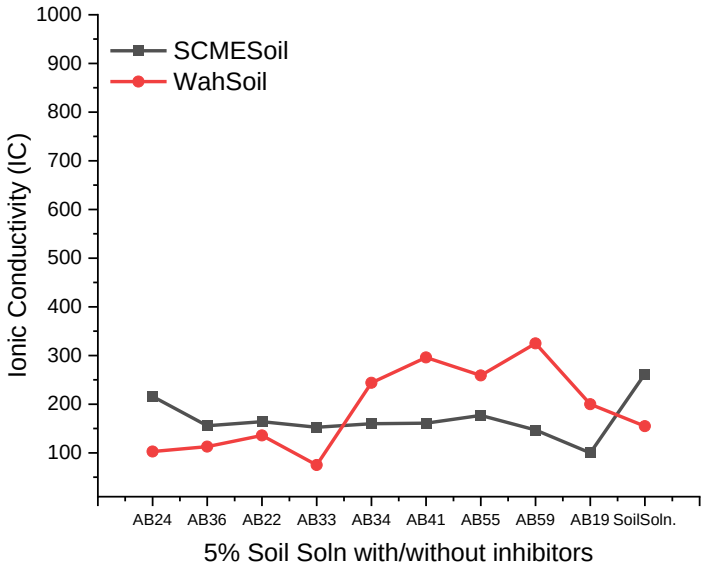

Figure 4.2: Ionic Conductivity Measurement of SCME and Wah soil soln. in the presence and absence of Schiff base inhibitors

4.1.3. Total dissolved Solids

The results of total dissolved solids measured using the TDS meter are shown in Table-4.3. The range of TDS measured using digital meter 41 to 208 mg/l. According to studies, the TDS value increases with the increment of the depth the soil sample has been taken. Hence, in the present study, we have taken samples from the depth of 125 cm. As per study [72], at a 600-700 cm depth, the TDS values are 400-500 mg/l. In the same study, the soil collected from the depth 164 cm the depth TDS was reported as 65 mg/l. Lower than 50 mg/l TDS is considered a corrosive environment because, at this value, the pH of the solution is reduced. Furthermore, the Ionic conductivity and TDS of the soil solutions are directly linked as the excess of conductive solids in the electrolyte would increase corrosion change. Thus, a similar trend is seen in the Ionic conductivity values and the values of the total dissolved solids.

Moreover, Figure-4.3 also illustrated the behaviour of different inhibitors used to create the environment that would reduce the corrosivity of the structure. Among the inhibitor-based solutions, only inhibitors of code AB33, AB22, AB36 and AB19 showed a reduction in the TDS, making it a less corrosive environment than the 5% soil solution environment.

Table 4.3: Ionic Conductivity Measurement of SCME and Wah soil soln. in the presence and absence of Schiff base inhibitors

Inhibitor based 5% soil soln.	SCME soln. TDS (mg/l)	WAH soln. TDS (mg/l)
AB24	129.3	61.2
AB36	91.5	68.5
AB22	98.5	81.32
AB33	91.9	44
AB34	89.4	151.90
AB41	96.5	176.9
AB55	107.1	157.6
AB59	89.8	208
AB19	60.3	121.5
5% Soil Solution	**168.5**	**91.5**

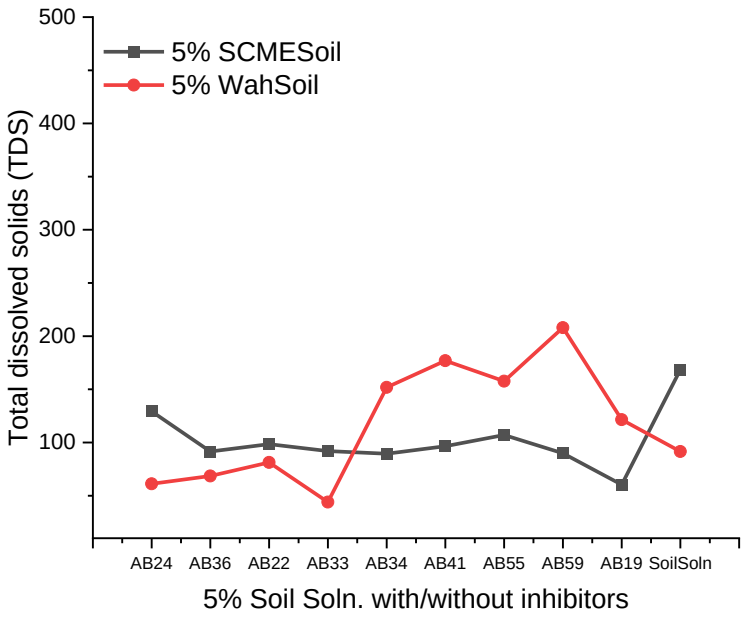

Figure 4.3: Ionic Conductivity Measurement of SCME and Wah soil soln. in the presence and absence of Schiff base inhibitors

Corrosivity measurements illustrated that the environment of the soil solution is inclined toward the acidic behaviour and thus can be labelled as the corrosive environment, which can be deteriorating for the walls of the carbon steel structure. Whereas the inhibitors of code AB33, AB22, AB36 and AB19 reduced corrosion, creating constituents in the environment.

4.2. Soil Resistivity Measurements

The probes distances were varied from 5 feet to 15 feet for each site, which collectively covered the 60 feet area of the total field. A battery was connected to the soil resistivity measuring equipment, and two probes, 1 and 4, were connected to obtain current, whereas the two inner probes were used to measure the voltage. Then the conversion of feet to meters was done, and then the soil resistivity was automatically measured by the equipment in ohmmeters. Usually, the soil resistivity equipment can measure the resistance. Therefore resistivity is calculated using the given Eq.11 [62]:

$$\rho = 2\pi AR \quad (11)$$

Where ρ is resistivity, A represents the distance between the probes, and R represents the soil resistance. The resistivity measurement is repeated for each 'A'. The average resistivity is considered the field soil resistivity. In Table-4.4, Table-4.5, and Table-4.6, the results of field one, field two and field three are recorded, respectively.

Table 4.4: First field soil resistivity results

Area (ft)	I (mA)	R(ohm)	Resistivity (ohm.m)
5	-443.5	1.446	13.839
10	471.2	0.434	8.3073
15	493.9	0.492	14.126
20	507.8	0.272	10.439

Average field resistivity = (13.839+8.3073+14.126+10.439)/4

ρ = 11.677825 ohm.m

ρ = 1167.78 ohm.cm

Table 4.5: Second field soil resistivity tests

Area (ft)	I (mA)	Average I(mA)	R (ohm)	Avg. R(ohm)	ρ(ohm.m)
5	-535.1		1.607		15.5697
10	-568.3		1.062		20.339
15	-555.3	550.5	788.9	0.7881	22.63
15	545.7		787.4		
20	541.6	536.3	551.8	0.5473	20.963
20	531.0		542.8		

Average field resistivity = (15.5697+20.339+22.63+20.963)/4

ρ = 19.875 Ω.m

ρ = 1987.5 Ω.cm

Table 4.6: Third field soil resistivity tests

Area (ft)	I (mA)	Average I(mA)	R (ohm)	Avg. R(ohm)	ρ(ohm.m)
5	527.6	531.3	1.831	1.826	17.682
5	535.0		1.821		
10	580.1	582.6	1.202	1.198	22.953
10	585.1		1.195		
15	570.1	572.8	0.873	0.8704	25.003
15	575.5		0.867		
20	567.3	569.5	0.601	0.600	22.98
20	571.7		0.598		

Average field resistivity = 17.682+22.953+25.003+22.98/4

ρ = 22.13 Ω.m

ρ = 2213 Ω.cm

Then results show that the resistivity of field 1 is 1167.78 ohm. cm, field 2 is 1987.5 ohms. cm**,** and the result of average soil resistivity of field 3 is 2213 ohm. cm. In Figure-4.4, the soil resistivity of each field comes under the range of 1000-3000 ohm. cm, which according to the literature, is considered as highly corrosive soil.

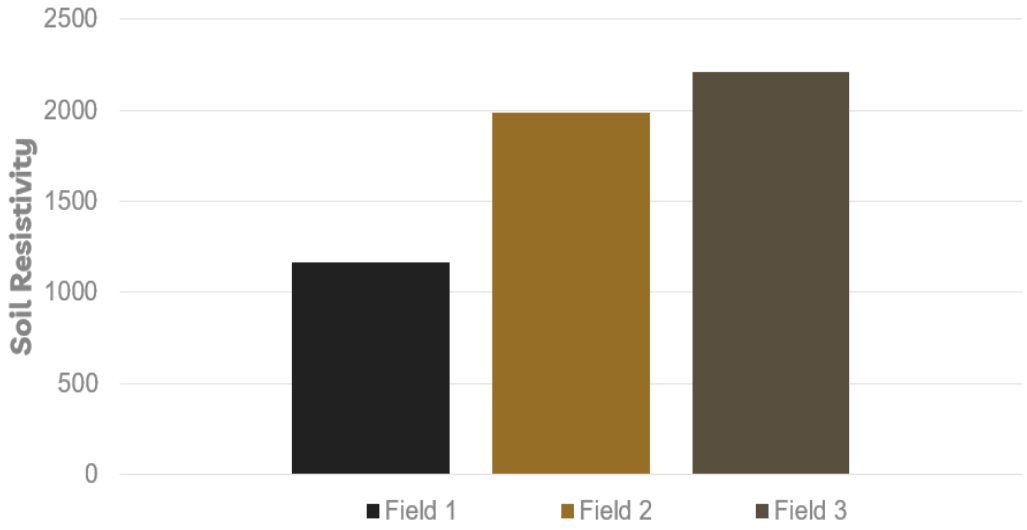

Figure 4.4: Graphical representation of the soil resistivity of three experimental fields

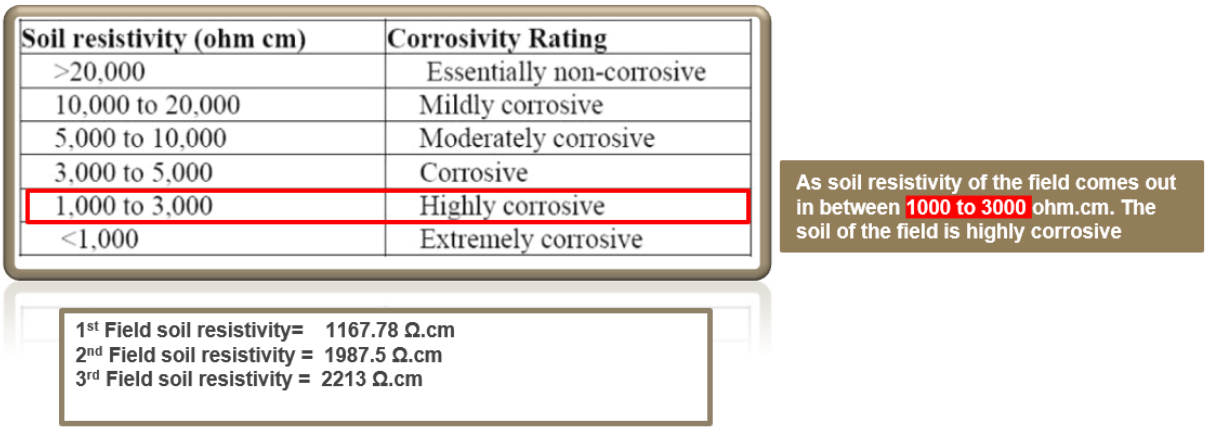

Figure 4.5: Soil resistivity as per literature [32]

Figure-4.5 shows that if the soil resistivity is more significant than 20,000 ohms.cm, the soil will be essentially non-corrosive, whereas if it is smaller than 1000 ohm. cm will be highly corrosive. However, the experimental field soil results came out to be under the range of 1000-3000 ohm.cm, which shows that the soil resistivity of the given field was less. Thus, the soil is highly corrosive and can damage the structure buried inside it.

4.3. Weight Loss Measurements

Monitoring the corrosion of metallic specimens is possible using the cross-section area of the sample as an indicator, where the difference between the weight of the specimen before and after immersion in the solution is used to calculate the corrosion rate.

Eq. 12 is used to calculate the corrosion rate using the weight difference of the specimen. However, for the long-term prediction of the weight loss, a logarithmic equation was proposed to predict the weight loss[73, 74]. The logarithmic equation is given below:

$$\ln(W_L) = a[\ln(t)] + b \tag{12}$$

'a' presents the slope of the linear Eq. 12, b indicating the y-intercept of the slope and *t* is the immersion time. However, N. Ali et al. [63] developed an equation that can substitute *ln* in Eq. 12. The equation was developed by plotting the slope in Table-4.7

against NaCl and soil solution concentration, which provides a strong relationship of linear regression $R^2 = 1$. The line equation of the plot can be written as:

$$a = (6.66\ x\ 10^{-6})C + (6.66\ x\ 10^{-6}) \quad (13)$$

By substituting the value of *'a'* in Eq. 12, the *ln* of the equation can be removed, and it would become Eq.14:

$$W_L = [(6.66\ x\ 10^{-6})C + (6.66\ x\ 10^{-6})]t + b \quad (14)$$

The above Eq.14 assisted us to calculate the weight loss of the carbon steel specimen immersed in a solution of NaCl and soil solution at any given time. Furthermore, the empirically modelled data specifically for weight loss measurement was validated by overlapping the experimental data and modelled data trend lines, showing that the modelled and experimental values are almost similar[75].

Table 4.7: Weight change of the carbon steel against the immersion time

T(h)	**W_L (mg)**			
	3.5% NaCl	**5% Soil Soln.**	**10% Soil Soln.**	**15% Soil Soln.**
480	0.0625	0.09952	0.1852	0.2725
960	0.0754	0.1156	0.2121	0.3021
1440	0.089	0.1385	0.2322	0.3512

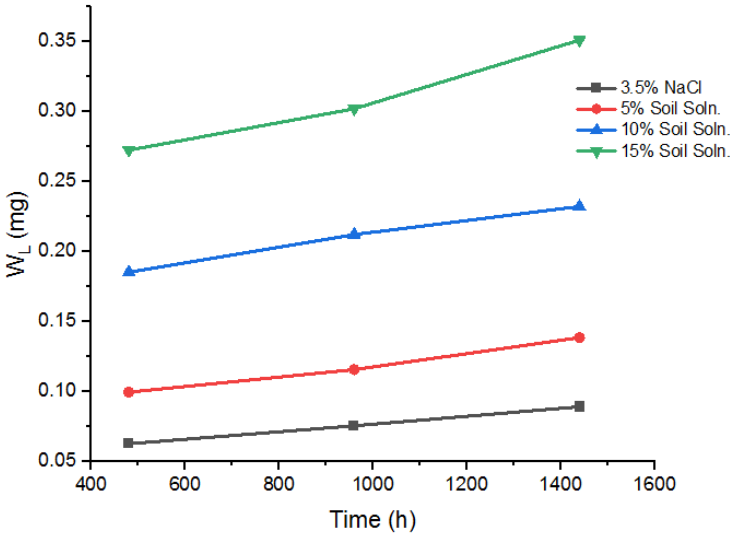

Figure 4.6: Plot of weightloss (W_L) versus Immersion time (h)

Table 4.8: Values of a (slope) and b(intercept) in the Eq.12

Concentration (%)	**a(mg/h)**	**b(mg)**	**R^2**
3.5	2.7e-5	0.04913	0.9997
5	4.06e-5	0.07889	0.9899
10	4.89e-5	0.16283	0.99307
15	8.19e-5	0.2299	0.97995

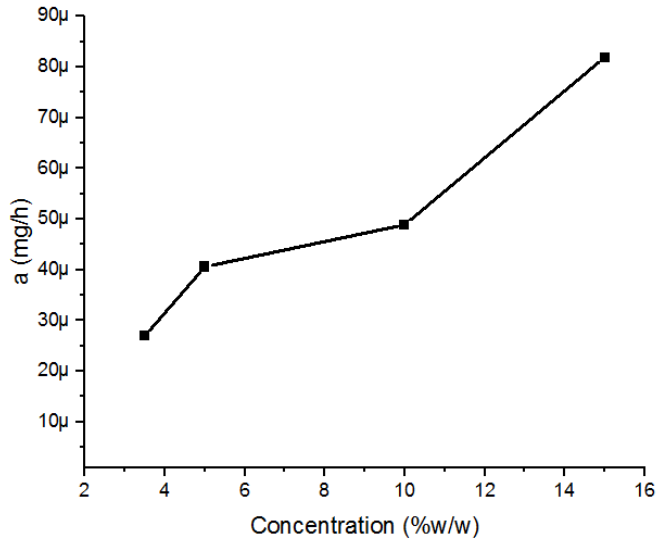

Figure 4.7: plot of slope (a) and concentration (%w/w)

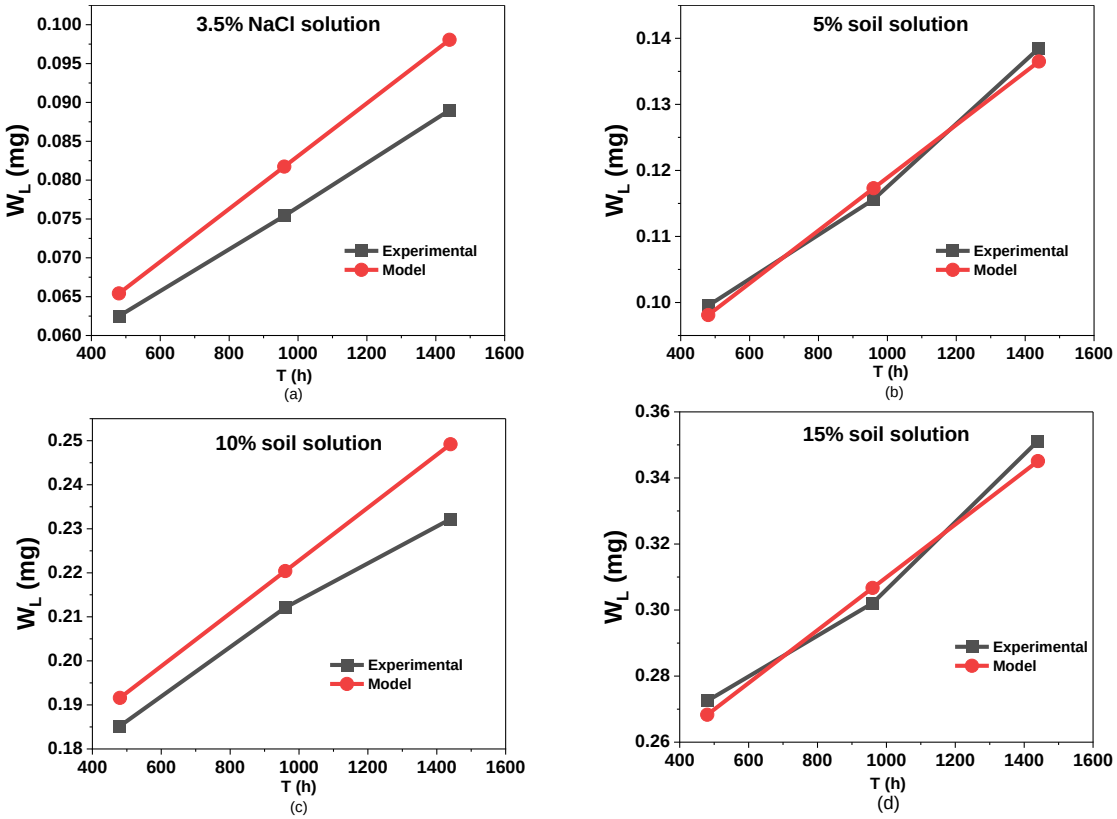

Figure 4.8: Curves of immersion time t(h) plotting against the weight change (W_L) in the four mediums with different concentrations (a) 3.5% NaCl Solution (b) 5% soil solution (c) 10% soil solution and (d) 15% soil solution

Table 4.9: Weight change of carbon steel against the immersion time

T(h)	W_L (mg)							
	3.5% NaCl		5% Soil Soln.		10% Soil Soln.		15% Soil Soln.	
	Exp	Model	Exp	Model	Exp	Model	Exp	Model
480	0.0625	0.06542	0.09952	0.0981	0.1852	0.1916	0.2725	0.2683
960	0.0754	0.08174	0.1156	0.1173	0.2121	0.2204	0.3021	0.3067
1440	0.089	0.09806	0.1385	0.1365	0.2322	0.2492	0.3512	0.3451

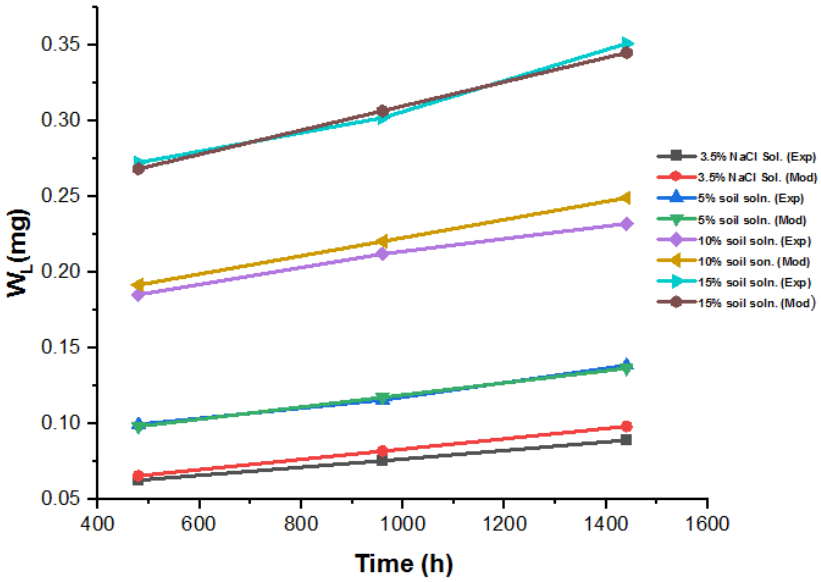

Figure 4.9: Plot of Experimental and Modelled data of Weight loss against time

By analyzing the results shown in the Figure-4.9, which shows the weight change of the carbon steel with the increase of immersion time – both experimentally and values obtained through modelling results, it illustrates that the 3.5% NaCl 5%, 10% and 15% soil solutions' concentrations or the compositions are making difference and thus the increase in weight change has been witnessed in the case of 5%, 10% and 15% soil solutions' as compared to the 3.5% NaCl solution. The simulation done using Eq. 15 can predict the weight loss of the carbon steel in the aqueous solution at any given concentration and time. The composition and morphology of the corrosion product can

be differed by the dissolved oxygen in any given aqueous solution carbon steel is immersed [76, 77].

Table 4.10: Corrosion rate against immersion time

T(h)	Cr (mpy)			
	3.5% NaCl	**5% Soil Soln.**	**10% Soil Soln.**	**15% Soil Soln.**
480	0.0387	0.0565	0.110	0.162
960	0.0445	0.0687	0.126	0.179
1440	0.0529	0.0823	0.138	0.208

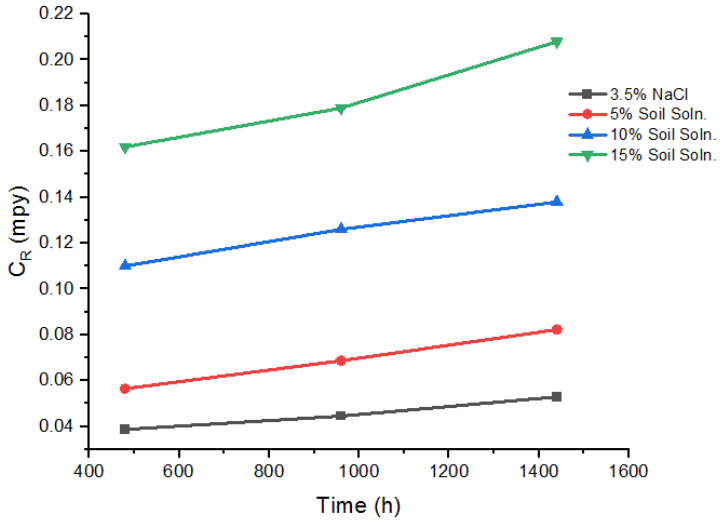

Figure 4.10: Plot of Corrosion Rate against Concentration

The chemical actions during the carbon steel immersion have induced a specific corrosion rate. The attack of corrosion happens to be on the surface of the immersed sample in the soil solution. Using Eq. 9, the calculation of the cross-section area of the specimen was performed, and the corrosion rate was calculated experimentally using Eq. 10. Also, the theoretical calculation of W_L was executed using Eq. 14. The corrosion rate of the specimen is illustrated in Figure-4.10, which shows the curves of Cr against t(h). Each curve shows that the corrosion is increasing in both cases, and that is what literature is predicting that the corrosion rate will increase to some extent in the given period and then tends to decrease. However, the corrosion rate is influenced by the salts and Cl^- ion present due to it.

Moreover, it is highly affected due to the bacterial entity present on the surface [78, 79]. As the empirical study is based on the soil solution concentration, the probability of bacterial bodies and the deterioration due to salt present in the soil increases by increasing the concentration. The increasing number of Cl^- ions in the solution will damage the passive layer, reducing the corrosion rate; as mentioned before, the corrosion rate will speed up more than ever [80]. During the corrosion process, both anodic and cathodic reactions occur, Fe^{-2} ions are slipping into the solution, and the electrons are left on the carbon steel surface. On the other hand, those free electrons present on the surfaces are gained by the H_2O and O_2 molecules while reducing [81]. Like the theoretical calculation of W_L of the carbon steel, the theoretical calculation of carbon steel is also possible using the concentration values, for the purpose the values of CR were plotted against the concentration 'C', the regression R = 1 of it shows that these two values are having solid relationships with each other. The following Eq.15 can be attained from the plot:

$$C_R = 0.0196C - 0.0157 \quad (15)$$

Using the above Eq.15, the corrosion rate can be identified of the sample at any soil solution concentration. However, at the specific concentration of the soil solution, the sample will fail, and thus it is observed that only the limited number of concentration values can be experimentally tested. Whereas the lifetime of the sample can be

calculated using Eq. 15 as, under a specific concentration of the soil solution and NaCl solution, concentration is the vital thing in an aqueous solution [82].

4.3.1. Potentiodynamic Measurements of Carbon steel in 3.5% NaCl, 5%,10% and 15% Soil Solution

The potentiodynamic study was carried out on the carbon steel sample 1040. The weight-loss study was performed to confirm and compare the corrosion rate obtained from the experimental study with the electrochemical analysis. The Table-4-11 shows the corrosion current densities and the corresponding corrosion rates in the 3.5% NaCl, 5%, 10%, 15% Soil Solution.

Table 4.11: Comparison of the electrochemical analysis of carbon steel sample observed in four different mediums.

Name of media	Concentration (%)	Current density $_{or}$/nA cm^{-2}	CR (e-3 mpy)	Weight loss method CR (e-3 mpy)
NaCl	3.5	50.55	22.84	38.7
Soil Soln.	5	90.55	41.3	56.5
Soil Soln.	10	192.90	53.46	110.1
Soil Soln.	15	276.52	126.34	162.5

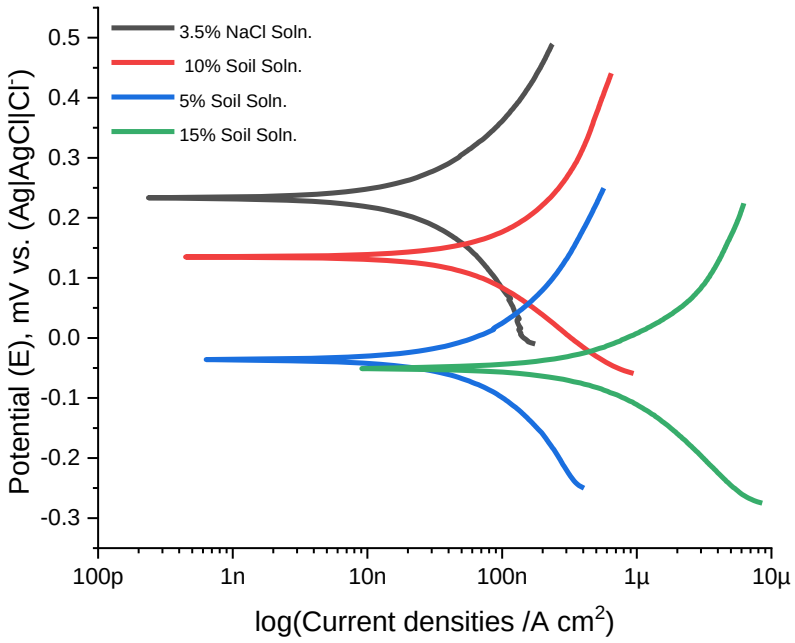

Figure 4.11: Tafel plots comparison of 3.5% NaCl, 5,10 and 15% Soil Solution

As shown in Figure-4.11, the Tafel plots illustrate that the 15% soil solution, which shows the highest current density value 125.5 $nAcm^{-2}$ among other concentrations and corrosion rate 0.126 mpy, complementing the corrosion rate obtained from weight loss which was 0.162 mpy. Similarly, the corrosion rate attained in the weight loss method for 5% solution was 0.038 mpy, and the corrosion rate acquired from the potentiodynamic study was 0.023 mpy. Furthermore, 3.5% NaCl and 10% Soil Solution value of carrion rate in potentiodynamic study and wright loss experiment verify the results.

4.4. Potentiodynamic polarization Measurements

Table 4.12: Corrosion tests data from Tafel plots of carbon steel in 5% SCME soil solution, with and without inhibitors.

Inhibitors Code	Concentration (mmol l^{-1}) e^{-3}	Current density $_{or}$/nA cm^{-2}	β_a (mV e^{-3})	- β_c (mV e^{-3})	CR (e-3 mpy)	Surface coverage (Θ)	The inhibition efficiency (Ɛ%)
Blank	-	60.53	176	205	27.48	-	-
AB24	1.099	29.45	101	142	13.46	0.52	52.42
AB36	1.107	20.79	106	125	9.50	0.64	64.42
AB22	1.123	50.33	130	131	23.01	0.18	18.66
AB33	1.089	26.61	140	154	12.16	0.57	57.00
AB34	0.937	50.12	111	134	22.91	0.19	19.00
AB41	1.214	49.94	112	142	22.82	0.19	19.34
AB55	1.151	44.61	90.5	99.9	20.38	0.27	27.96
AB59	1.124	42.89	109	140	19.61	0.30	30.68
AB19	1.044	29.43	178	183	13.45	0.52	52.45

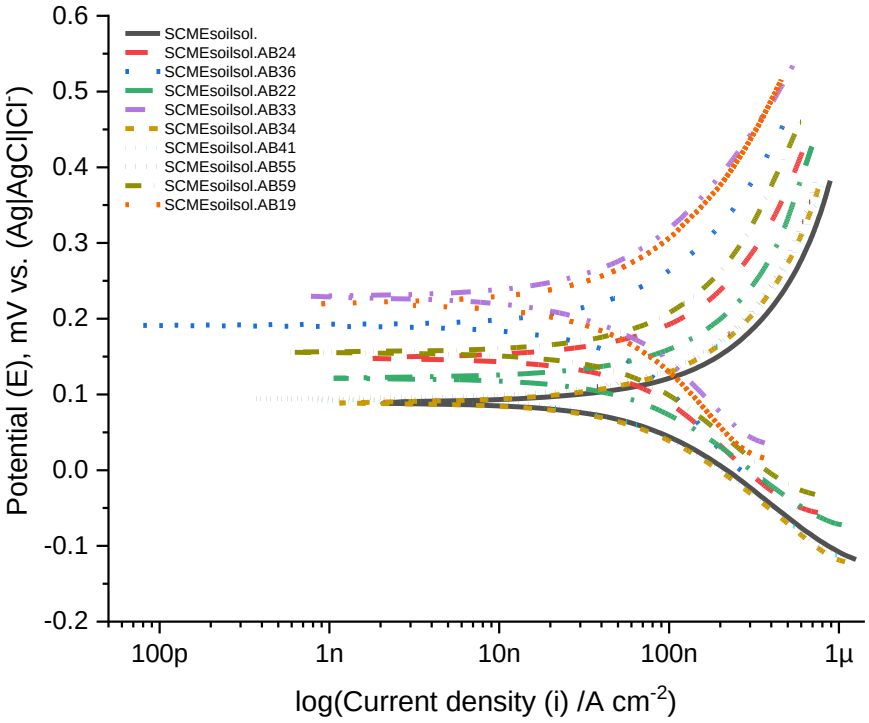

Figure 4.12: Superimposed Tafel analysis curves of the Schiff base inhibitors in the SCME soil soln. environment

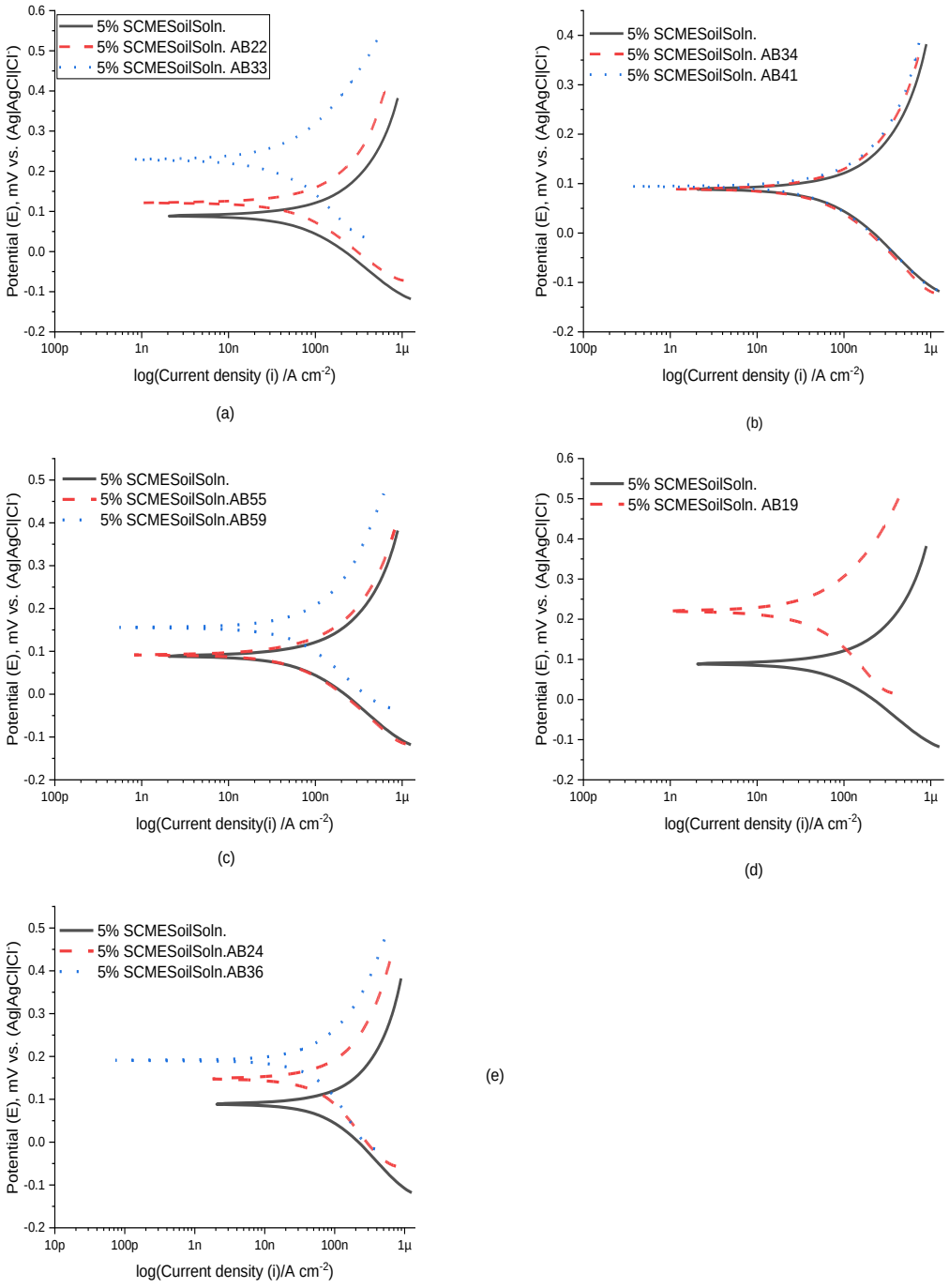

Figure 4.13: Tafel analysis curves of the carbon steel, the different overlapped graph of SCME soil solution as an electrolyte without and with inhibitor (a) AB22 and AB33 (b) AB34 and AB41 (c) AB55 and AB59 (d) AB19 (e) AB24 and AB36

Table 4.13: Corrosion tests data from Tafel plots of carbon steel in 5% Wah soil

Inhibitors Code	**Concentration (mol l^{-1}) e^{-3}**	**Current density i_{corr}/nA cm^{-2}**	**β_a (mV e^{-3})**	**- β_c (mV e^{-3})**	**CR (e-3 mpy)**	**Surface coverage (Θ)**	**The inhibition efficiency ($Z\%$)**
Blank	-	70.38	102	129	28.9	0	0
AB24	1.099	43.64	98.7	140	13.46	0.38	38.0
AB36	1.107	67.66	80.5	152	9.50	0.03	3.88
AB22	1.123	20.65	138	133	23.01	0.70	70.6
AB33	1.089	33.63	82.6	120	12.16	0.52	52.2
AB34	0.937	30.22	113	130	22.91	0.57	57.07
AB41	1.214	46.03	102	99.7	22.82	0.34	34.59
AB55	1.151	35.06	99.7	98.0	20.38	0.50	50.20
AB59	1.124	51.5	95.8	112	19.61	0.26	26.8
AB19	1.044	41.59	132	163	13.45	0.40	40.90

solution, with and without inhibitors.

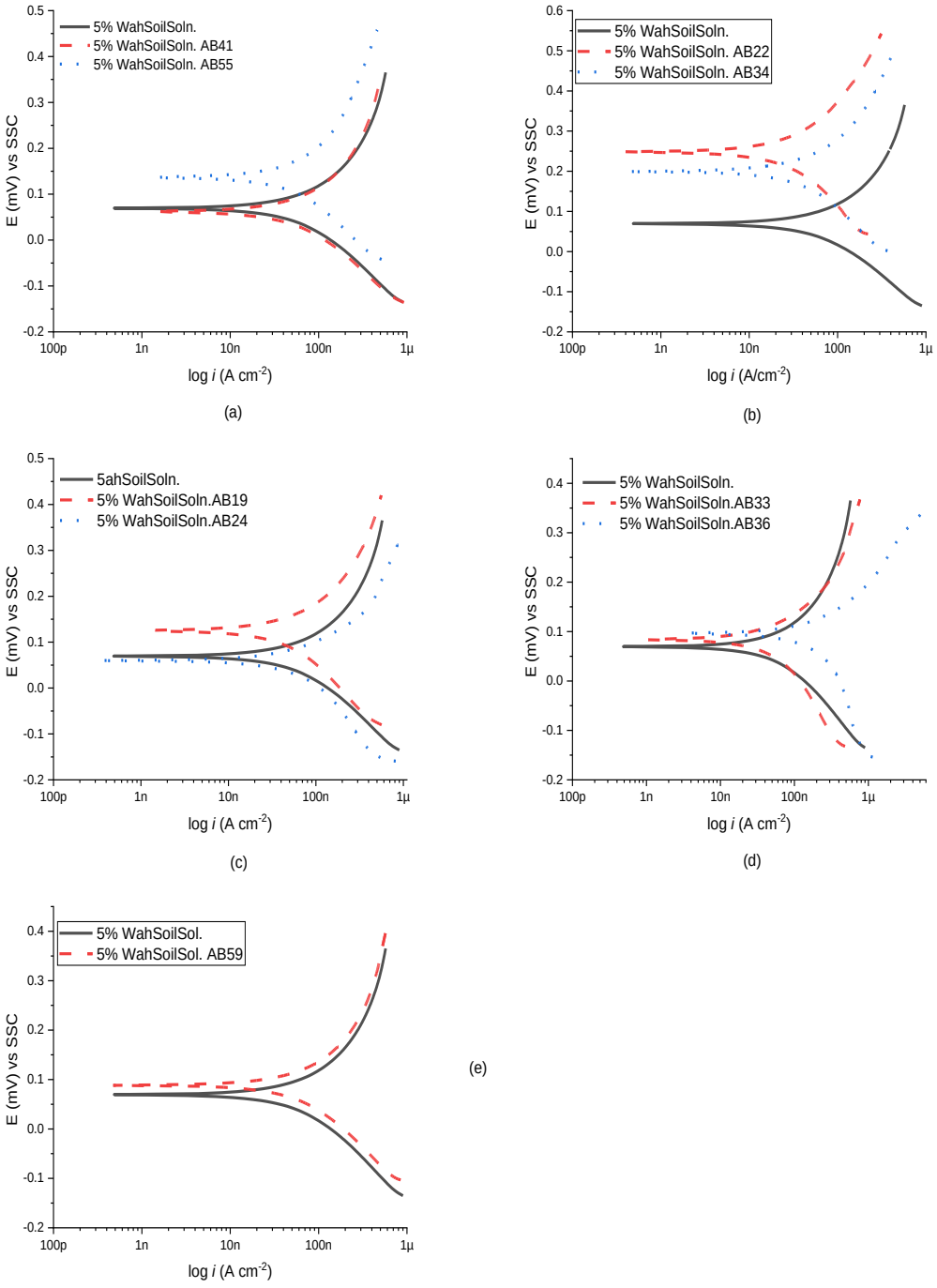

Figure 4.14: Tafel analysis curves of the carbon steel, the different overlapped graph of Wah soil solution as an electrolyte without and with inhibitor (a) AB41 and AB55 (b) AB22 and AB34 (c) AB19 and AB24 (d) AB33 and AB36 (e) AB59

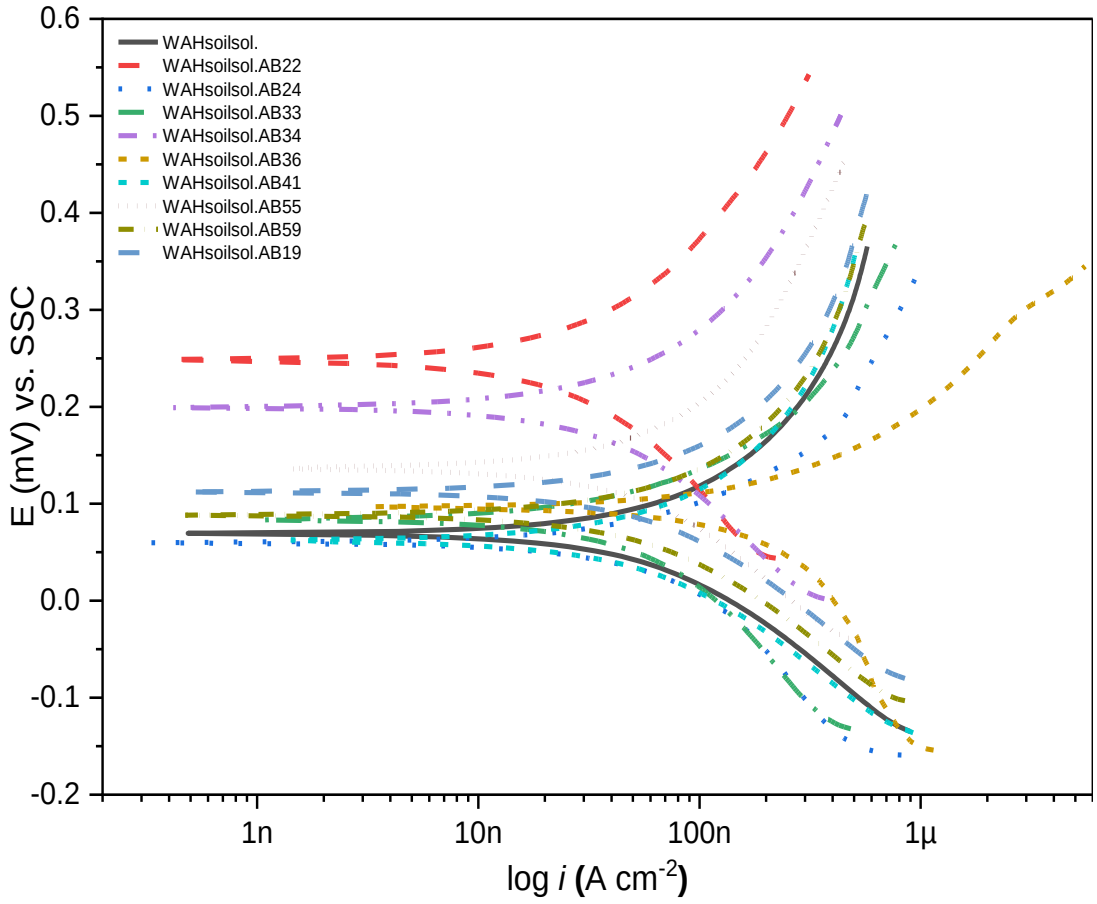

Figure 4.15: Polarization curves of the Schiff base inhibitors in the Wah soil 5% solution environment

The potentiodynamic polarization measurement curves are shown in Figure-4.12. These curves are for the carbon steel specimens in the 5% soil (SCME) solution and in the presence of nine Schiff bases inhibitors. The Tafel regions define the anodic and cathodic polarization curves prominently in the soil base aqueous solution in which the performance of inhibitors has been investigated. In Figure-4.12, the decrement of the anodic and cathodic currents is quite visible after the incorporation of Schiff base inhibitors, in which the AB24, AB36, AB33 and AB19 are showing quite good performance. Also, reducing the anodic, cathodic current can be arranged where AB36 outperforms and has effectively shown reduced current values. The effect is due to the

retardation of hydrogen evolution reaction and the reduction of anodic dissolution of carbon steel due to inhibitor[83]. The behaviour complements the efficiency of inhibitors on the sites of metal that actively assist the adsorption of inhibitors. However, AB22 has shown the low performance highest corrosion current value [84].

In Figure-4.15, the results of potentiodynamic measurements of carbon steel in 5% soil (Wah) solutions were studied first in the absence of inhibitors and then by incorporating inhibitors in the solution. As the carbon steel exposed to the Schiff based inhibitors, some of them have shown the suppression of anodic, cathodic current. However, some of them, like AB36, shown the lowest performance in the environment, although the decrease in the cathodic and anodic current is visible due to the inhibitors compared to the blank solution. Whereas discussed in the case of SCME soil solution base Tafel plots, there are some of the inhibitors in the 'Wah soil' environment like AB22, AB33, AB34 and AB55 shown receded values of anodic and cathodic current; due to the blockades on the active sites of the carbon steel sample occurring because of the inhibitors' adsorption on the surface [83].

The extrapolation of the Tafel lines to the corrosion voltage (E_{corr}) assisted in obtaining the corrosion current density (I_{corr}). The corrosion rate was then calculated using the determined corrosion density with the help of Tafel plots, using the following Eq.16:

$$Corrosion\ Rate = CR = \frac{(I_{corr}).(K)(\omega)}{(\alpha)(d)} \tag{16}$$

Where $_{Your}$ is current density, *K* is corrosion rate constant for mills per year it is 1.288 x 10^5 mm (A-cm-year), ω depicts equivalent weight, α is surface area, and *d* is density. However, efficiency (Ɛ%) of the inhibitors and the surface coverage degree (Θ) of the mentioned Schiff bases inhibitors were calculated using the Eq.17 given below:

$$Ɛ\% = \frac{I_{Corr.Uninhibited} - I_{Corr.Inhibited}}{CR_{Corr.Uninhibited}}\ x\ 100 \tag{17}$$

$$\theta = \frac{I_{Corr.Uninhibited} - I_{Corr.Inhibited}}{I_{Corr.Uninhibited}} \tag{18}$$

Here, $I_{Corr.Uninhibited}$ and $I_{Corr.Inhibited}$ are representing the Uninhibited and inhibited corrosion currents. The inhibited corrosion currents are those calculated using the Tafel extrapolation. In contrast, the inhibitors under consideration and the uninhibited corrosion currents are measured utilizing the Tafel extrapolation of data obtained from the blank 5% soil solution before adding inhibitors. Table-4.12 and Table-4.13 are representing the corrosion parameters for the SCME and Wah environment, including the slopes of the cathodic and anodic Tafel curve, the slopes (β_c) and (β_a) calculated using the Gamry Echem Analyst program, Current density (I_{corr}), inhibition efficiency percentage (Ɛ%). Table-4.12 and Table-4.13 illustrate that the changes have been observed in both slopes (β_c) and (β_a) after adding Schiff base inhibitors. The Tafel slope (β_c) is greater than the anodic slope in both cases. Hence, the corrosion kinetics under the soil solution is controlled by cathode, primarily. The parallel cathodic curves support this argument. Even after the addition of the inhibitors, the hydrogen evolution is happening as a reduction reaction on the surface of the specimen, and charges are still being transferred. Table-4.12 and Table-4.13 also show that the corrosion current density declines as the inhibition efficiency (Ɛ%) increases. The results show that the Schiff base inhibitors molecules adsorbed on the specimen's surface on mutually cathodic and anodic sites. Nevertheless, the lowest recorded decrease in corrosion current density value was reflected for the AB22 in the Wah soil solution environment. This represents the three possible reasons that aided the coverage: molecular size, number of active sites, and the increment of electron densities. The values of corrosion potential E_{corr} are mostly shifting toward the cathodic direction, which shows that it is the 5% soil solution trend, so based on these facts, it can be quoted as the characteristics of the cathodic shift E_{corr} represents the cathodic behaviour of the inhibitor. The shift's occurrence indicates the blockade emerges due to the adsorption on active sites after adding inhibitor in the solution [85]. The reaction on the surface of the specimen to be tested is the same before and after the addition of the inhibitor. Hence, the change on E_{corr} represents that the active sites have been variation after the inhibitors are added, and thus the corrosion rates have been differing. Moreover, the coverage value of the inhibitors closer to 1 can be called as they provide good coverage with the assistance of the adsorbed layer of inhibitors on the surface [86, 87]. Hence, the higher the value of

coverage, the better the shielding property of the inhibitor, which can significantly protect the surface by declining the corrosion rate of carbon steel, prominently [88, 89]. According to the efficiency of the inhibitors in the SCME soil environment, it can be arranged as AB36>AB33>AB19>AB24. Whereas, for the Wah soil solution environment, the efficiency of the inhibitor can be arranged as AB22>AB34>AB33>AB55. The efficiencies calculated using the polarization curves are then compared with the Linear polarization curves, showing good similarity between the values calculated using Tafel analysis.

4.5. Linear Polarization Resistance

Table 4.14: LPR measurements of selective Schiff base inhibitors in the 5% SCME soil solution

Inhibitor Code	**Concentration (mol l^{-1}) e^{-3}**	**R_p (ohms)**	**I_{corr} (nA)**	**Corrosion Rate (e^{-3}mpy)**	**Surface Coverage*(Θ)***	**The inhibitor efficiency *(Ɛ%)***
Blank	-	453.854	57.47	26.26	-	-
AB19	1.044	761.464	34.25	15.65	0.43	43.56
AB33	1.089	721.596	36.15	16.52	0.40	40.30
AB34	0.937	979.714	26.60	12.15	0.56	56.69

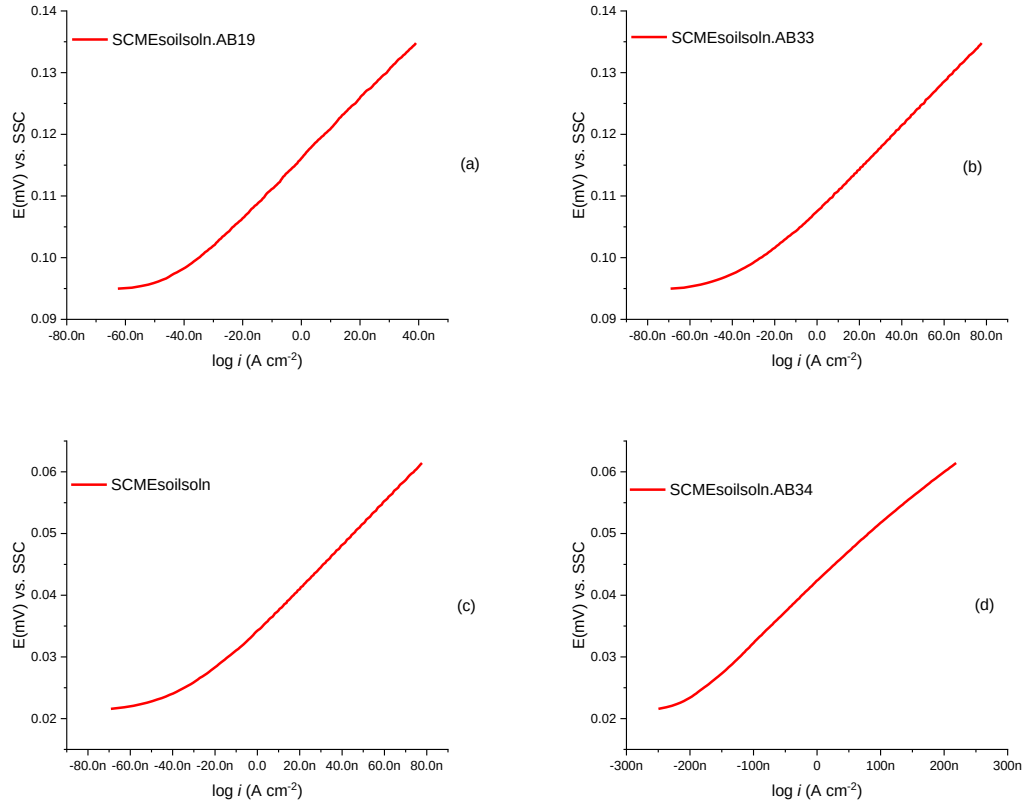

Figure 4.16: LPR curves of the carbon steel, SCME soil solution as an electrolyte with and without Schiff base inhibitors. Three graphs are with inhibitors (a) AB19, (b) AB33 and (d) AB34. Whereas (c) representing without inhibitor SCME soil soln.

Table 4.15: LPR measurements of selective Schiff base inhibitors in the 5% Wah soil solution

Inhibitor Code	**Concentration (mol l^{-1}) e^{-3}**	**R_p (kohms)**	**I_{corr} (nA)**	**Corrosion Rate (e^{-3}mpy)**	**Surface Coverage(Θ)**	**The inhibitor efficiency ($\mathcal{E}$%)**
Blank	-	419.961	60.21	27.52	-	-
AB19	1.044	873.597	29.86	13.64	0.52	52.33
AB33	1.089	813.329	32.07	14.65	0.48	48.52
AB34	0.937	844.259	30.89	14.11	0.50	50.56

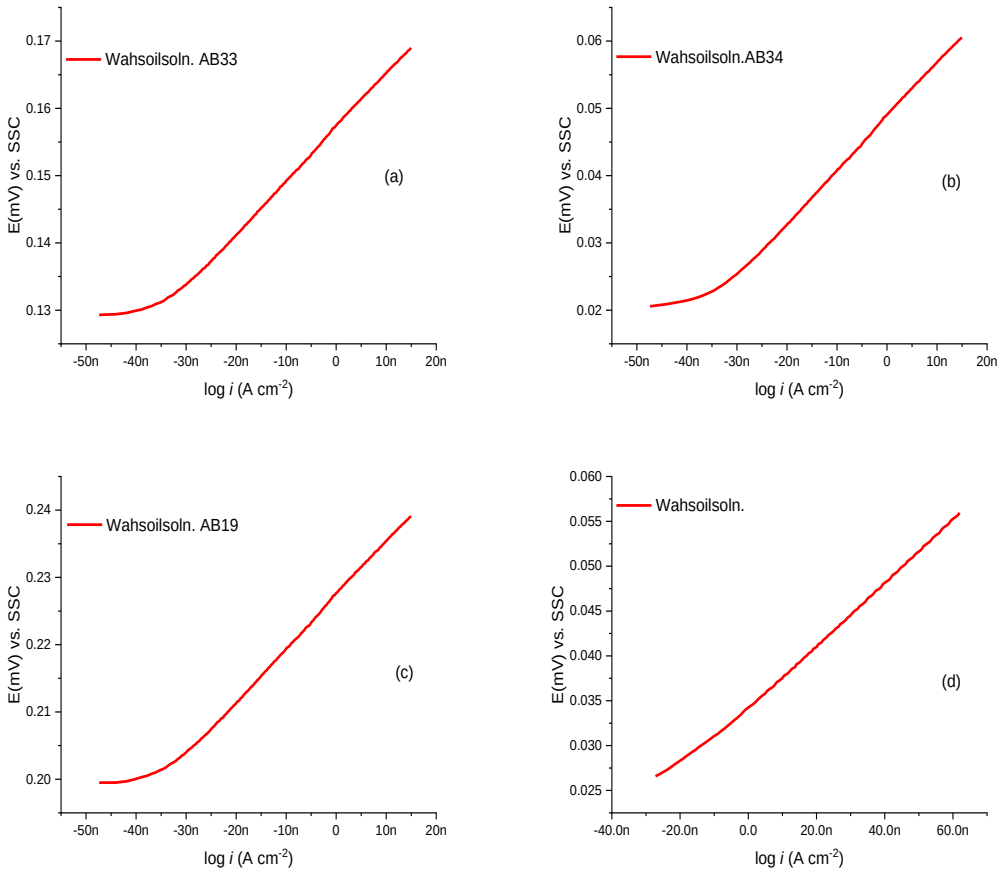

Figure 4.17: LPR curves of the carbon steel, Wah soil solution as an electrolyte with and without Schiff base inhibitors. Three graphs are with inhibitor (a) AB33, (b) AB34 and (c) AB19. Whereas (d) representing without inhibitor Wah soil soln.

The linear polarization is performed to verify the results of the Tafel analysis. Three inhibitors are preferred based on their performances in the given soil environments; the chosen inhibitors codes are AB19, AB33 and AB34. Electrolyte for the experiment was prepared using the soil of two locations and in the same way mentioned in the methodology section. The inhibitors were added before experimenting. The Linear polarization resistance results are shown in Figure-4.17 allows to calculate of the slope, which represents the polarization resistance R_p value, which provides the gateway to calculate the I_{corr}, [90] using the following Eq.19:

$$I_{corr} = \frac{(\beta_a \beta_c)}{(2.3)(R_p)(\beta_a + \beta_c)} \quad (19)$$

Where β_a and β_c are Tafel slopes according to the standards it is taken as $120e^{-3}$ V; value 2.3 is the part of the Stern-Geary coefficient B, given as:

$$B = \frac{(\beta_a \beta_c)}{(2.3)(\beta_a + \beta_c)} \quad (20)$$

The corrosion rate was calculated using Faraday's Eq.21 standard (ASTM G 59):

$$Corrosion\ Rate = CR = \frac{(I_{corr}).(K)(\omega)}{(\alpha)(d)} \quad (21)$$

Where $_{Your}$ is current density, *K* is corrosion rate constant for mills per year it is 1.288 x 10^5 mm (A-cm-year), ω depicts equivalent weight, α is surface area, and *d* is density. However, efficiency (Ɛ%) of the inhibitors and the surface coverage degree (Θ) of the mentioned Schiff bases inhibitors were calculated using the Eq.22 given below:

$$Ɛ\% = \frac{CR_{Uninhibited} - CR_{Inhibited}}{CR_{Uninhibited}}\ x\ 100 \quad (22)$$

$$\theta = \frac{CR_{Uninhibited} - CR_{Inhibited}}{CR_{Uninhibited}} \quad (23)$$

Here, $CR_{Uninhibited}$ and $CR_{Inhibited}$ are representing the Uninhibited and inhibited rate of corrosion. The inhibited corrosion rates are calculated using the determined current densities. The inhibitors under consideration and the uninhibited corrosion rates are calculated utilizing the current densities determined in the blank 5% soil solution before adding inhibitors. From Table-4.14 and Table-4.15, the R_p is recorded as lowest when the electrolyte without inhibitor was utilized for executing Linear polarization resistance measurements; on the other hand, the R_p of the inhibitor AB34 in both environments was noted slightly higher. The relation of polarization resistance R_p is inverse with corrosion current density I_{corr}. Thus, the values of $_{Icorr}$ against the lower R_p values are higher than those with higher R_p values. However, comparing the current densities observed in Tafel analysis of the nominated inhibitors and the current density values noted in the Linear polarization resistance method makes a good agreement. The corrosion rate of the specimen without the inhibitor, as illustrated in Figure-4.16c,

increases with time because iron carbide is producing on the surface of the specimen as a result of corrosion reactions, and further allowing increasing the surface area for the cathodic reaction that catalyzes corrosion rate [91]. Moreover, the increment of corrosion rate CR is affiliated to the decrement of the pH and the launch of the galvanic effect amongst cementite and ferrite phase present in the non-oxidized state of carbon steel and due to dissolution of ferrite into Fe^{2+} the layer of cementite form on the surface of the specimen [92].

Using Eq.22, the efficiency of the Schiff based inhibitors were calculated and using these inhibitors, the corrosion rate of carbon steel decreased notably by using the selected inhibitors in the solution. The corrosion rate CR in the presence of AB33 shows the mpy in the SCME medium and the Wah medium; it was reduced from the value 26.26 e-3 mpy to 16.25 e-3 mpy. Inhibition efficiencies increase by 40.30% and 46 % in SCME and Wah medium, respectively. Also, the surface coverage to the carbon steel specimen was 0.46 and 0.40 in Wah and SCME medium, respectively. Moreover, the declination in the corrosion rate and increment of inhibition and coverage was studied in the AB19 and AB34. The maximum efficiency noted in the experiment was 56% using inhibitor AB34 and the minimum according to the Linear polarization resistance was 40% using inhibitor AB33 in the medium SCME soil solution. These chosen Schiff base inhibitors have an excellent ability to protect and create the protective layer, even in the presence of only 300ppm [93].

Conclusions

1. The inhibitors investigated in the study was adequate for protecting carbon steel in the soil solutions.
2. The 'SCME soil' pH was relatively lower, whereas the ionic conductivity was relatively higher than 'Wah soil,' indicating that the SCME soil was relatively aggressive.
3. The corrosion rate of steel increased with immersion time in soil solutions, which was justified by modelling the experimental results and the potentiodynamic study.
4. The ‘E-log i’ curves shifted in anodic directions in the two soil solutions by incorporating inhibitors; the shift was more significant in ‘Wah soil’ compared with ‘SCME soil’ due to its higher corrosivity. In the 'SCME soil' environment the inhibitors of code ‘AB24’, AB36, AB33 and AB19 are showing quite good performance. Also, reducing the anodic, cathodic current can be arranged where AB36 is outperforming and has shown reduced current values effectively. In the ‘Wah soil’ environment, AB22, AB33, AB34 and AB55 showed receded values of anodic and cathodic current; due to the blockades on the active sites of the carbon steel sample because of the inhibitors adsorption on the surface.
5. According to the efficiency of the inhibitors in the ‘SCME soil’ environment, it can be arranged as AB36=64.42%>AB33=52.2%>AB19=40.90%>AB24=38% and the lowest efficiency was recorded for the inhibitor AB22=18.66%. Whereas, for the ‘Wah soil’ environment, the efficiency of the inhibitor can be arranged as AB22=70.6%>AB34=57.07%>AB33=52.20%>AB55=50.20%, and the lowest efficiency was for AB36 = 3.88%. The efficiencies calculated using the polarization curves are then compared with the Linear polarization curves, showing good similarity between the values calculated using Tafel analysis.
6. The linear polarization is performed to verify the results of the Tafel analysis. Three inhibitors are preferred based on their performances in the given soil environments; the chosen inhibitors codes are AB19, AB33 and AB34. The maximum efficiency noted in the experiment was 56% using inhibitor AB34 and the minimum according to the Linear polarization resistance was 40% using inhibitor AB33 in the medium

SCME soil solution. These chosen Schiff base inhibitors have an excellent ability to protect and create the protective layer, even in the presence of the only 300ppm.

References

[1] M. Abdelsattar, A. E.-F. M. Badawi, S. Ibrahim, A. F. Wasfy, A. H. Tantawy, and M. M. Dardir, "Corrosion Control of Carbon Steel in Water-Based Mud by Nanosized Metallo-Cationic Surfactant Complexes During Drilling Operations," *ACS omega,* vol. 5, pp. 30881-30897, (2020).

[2] M. Chigondo and F. Chigondo, "Recent natural corrosion inhibitors for mild steel: an overview," *Journal of Chemistry,* vol. 2016, (2016).

[3] Y.-S. Kim and J.-G. Kim, "Corrosion behavior of pipeline carbon steel under different iron oxide deposits in the district heating system," *Metals,* vol. 7, p. 182, (2017).

[4] F. S. Kadhim, "Investigation of carbon steel corrosion in water base drilling mud," *Modern Applied Science,* vol. 5, p. 224, (2011).

[5] L. T. Popoola, A. S. Grema, G. K. Latinwo, B. Gutti, and A. S. Balogun, "Corrosion problems during oil and gas production and its mitigation," *International Journal of Industrial Chemistry,* vol. 4, pp. 1-15, (2013).

[6] A. Pradityana, Sulistijono, A. Shahab, and S. Chyntara, "Eco-friendly green inhibitor of mild steel in 3, 5% NaCl solution by Sarang Semut (Myrmecodia Pendans) extract," in *AIP Conference Proceedings*, (2014), pp. 161-164.

[7] F. Suedile, F. Robert, C. Roos, and M. Lebrini, "Corrosion inhibition of zinc by Mansoa alliacea plant extract in sodium chloride media: extraction, characterization and electrochemical studies," *Electrochimica Acta,* vol. 133, pp. 631-638, (2014).

[8] S. Utami, M. Fermi, Y. Aziz, and R. Irianti, "Corrosion control of carbon steel using inhibitor of banana peel extract in acid diluted solutions," in *IOP Conference Series: Materials Science and Engineering*, (2018), p. 012030.

[9] M. A. El-Haddad, A. B. Radwan, M. H. Sliem, W. M. Hassan, and A. M. Abdullah, "Highly efficient eco-friendly corrosion inhibitor for mild steel in 5 M HCl at elevated temperatures: experimental & molecular dynamics study," *Scientific reports,* vol. 9, pp. 1-15, (2019).

[10] E. E. Oguzie, "Corrosion inhibition of aluminium in acidic and alkaline media by Sansevieria trifasciata extract," *Corrosion science,* vol. 49, pp. 1527-1539, (2007).

[11] M. Osman, A. Omar, and A. Al-Sabagh, "Corrosion inhibition of benzyl triethanol ammonium chloride and its ethoxylate on steel in sulphuric acid solution," *Materials Chemistry and Physics,* vol. 50, pp. 271-274, (1997).

[12] N. Negm, Y. Elkholy, M. Zahran, and S. Tawfik, "Corrosion inhibition efficiency and surface activity of benzothiazol-3-ium cationic Schiff base derivatives in hydrochloric acid," *Corrosion Science,* vol. 52, pp. 3523-3536, (2010).

[13] Y. Abboud, A. Abourriche, T. Saffaj, M. Berrada, M. Charrouf, A. Bennamara, *et al.*, "2, 3-Quinoxalinedione as a novel corrosion inhibitor for mild steel in 1 M HCl," *Materials chemistry and physics,* vol. 105, pp. 1-5, (2007).

[14] E. Garcia-Ochoa, S. Guzmán-Jiménez, J. G. Hernández, T. Pandiyan, J. M. Vásquez-Pérez, and J. Cruz-Borbolla, "Benzimidazole ligands in the corrosion inhibition for carbon steel in acid medium: DFT study of its interaction on Fe30 surface," *Journal of Molecular Structure,* vol. 1119, pp. 314-324, (2016).

[15] O. Obiukwu, I. Opara, and L. U. Grema, "Corrosion inhibition of mild steel by various plant extracts in acid media," *Research Journal of Applied Sciences, Engineering and Technology,* vol. 10, pp. 1197-1205, (2015).

[16] H. Wang, H. Yuan, S. Li, Z. Li, M. Jiang, and J. Tang, "Activity prediction of Schiff base compounds using improved QSAR models of cinnamaldehyde analogues and derivatives," *BioResources,* vol. 10, pp. 7921-7935, (2015).

[17] P. Shetty, "Schiff bases: An overview of their corrosion inhibition activity in acid media against mild steel," *Chemical Engineering Communications,* vol. 207, pp. 985-1029, (2020).

[18] A. Fouda, H. Megahed, N. Fouad, and N. Elbahrawi, "Corrosion inhibition of carbon steel in 1 M hydrochloric acid solution by aqueous extract of Thevetia peruviana," *Journal of Bio-and Tribo-Corrosion,* vol. 2, pp. 1-13, (2016).

[19] J. T. Nwabanne and V. N. Okafor, "Adsorption and thermodynamics study of the inhibition of corrosion of mild steel in H 2 SO 4 medium using Vernonia

amygdalina," *Journal of Minerals and Materials Characterization and Engineering,* vol. 11, p. 885, (2012).

[20] S. Şafak, B. Duran, A. Yurt, and G. Türkoğlu, "Schiff bases as corrosion inhibitor for aluminium in HCl solution," *Corrosion science,* vol. 54, pp. 251-259, (2012).

[21] H. M. A. El-Lateef, M. Ismael, and I. M. A. Mohamed, "Novel Schiff base amino acid as corrosion inhibitors for carbon steel in CO2-saturated 3.5% NaCl solution: experimental and computational study," *Corrosion Reviews,* vol. 33, pp. 77-97, (2015).

[22] A.-R. El-Sayed, A. M. Shaker, and H. M. Abd El-Lateef, "Corrosion inhibition of tin, indium and tin–indium alloys by adenine or adenosine in hydrochloric acid solution," *Corrosion Science,* vol. 52, pp. 72-81, (2010).

[23] M. Honarvar Nazari, M. S. Shihab, E. A. Havens, and X. Shi, "Mechanism of corrosion protection in chloride solution by an apple-based green inhibitor: experimental and theoretical studies," *Journal of Infrastructure Preservation and Resilience,* vol. 1, pp. 1-19, (2020).

[24] H. Ouici, M. Tourabi, O. Benali, C. Selles, C. Jama, A. Zarrouk, *et al.*, "Adsorption and corrosion inhibition properties of 5-amino 1, 3, 4-thiadiazole-2-thiol on the mild steel in hydrochloric acid medium: Thermodynamic, surface and electrochemical studies," *Journal of Electroanalytical Chemistry,* vol. 803, pp. 125-134, (2017).

[25] A. Bahadori, *Cathodic corrosion protection systems: a guide for oil and gas industries*: Gulf professional publishing, (2014).

[26] K. Davies and J. Broomfield, "Cathodic protection mechanism and a review of criteria," *Cathodic Protection of Steel in Concrete and Masonry,* vol. 41, (2013).

[27] E. Ameh and S. Ikpeseni, "Pipelines cathodic protection design methodologies for impressed current and sacrificial anode systems," *Nigerian Journal of Technology,* vol. 36, pp. 1072-1077, (2017).

[28] A. Ali, "Performance of Cathodic Protection for Pipe Lines," M. Sc. thesis, College of Engineering, Al-Nahrain University, (2014).

[29] D. Harvey, "Cathodic Protection (Guides to Good Practice in Corrosion Control No. 1)," (2019).

[30] A. I. EL-Alem, A. M. Azmy, and A. Hosam-Eldin, "DESIGN OF A CATHODIC PROTECTION SYSTEM TO PREVENT CORROSION OF METALLIC STRUCTURES USING HYBRID RENEWABLE ENERGY SOURCES," *ERJ. Engineering Research Journal,* vol. 36, pp. 109-117, (2013).

[31] L. Fan, S. T. Reis, G. Chen, and M. L. Koenigstein, "Corrosion resistance of pipeline steel with damaged enamel coating and cathodic protection," *Coatings,* vol. 8, p. 185, (2018).

[32] H. M. Saif Al Deen and I. M. Abdulbaqi, "Design and implementation of an impressed current cathodic protection system for buried metallic pipes (part II)(considering Al-Quds gas station in Baghdad)," *International Journal of Power Electronics and Drive Systems,* vol. 11, p. 275, (2020).

[33] K. Usher, A. Kaksonen, I. Cole, and D. Marney, "Critical review: microbially influenced corrosion of buried carbon steel pipes," *International Biodeterioration & Biodegradation,* vol. 93, pp. 84-106, (2014).

[34] F. A. V. Bazán and A. T. Beck, "Optimal design of buried pipelines considering failure by mechanical damage," *Structure and Infrastructure Engineering,* vol. 12, pp. 1477-1486, (2016).

[35] N. Rahman and M. Ismail, "Corrosion protection coating for buried pipelines: a short review," *World Applied Sciences Journal,* vol. 4, pp. 524-531, (2012).

[36] J. Villanueva-Balsera, F. Ortega-Fernandez, and F. Rodriguez-Perez, "Methods to evaluate corrosion in buried steel structures: A review," *Metals,* vol. 8, p. 334, (2018).

[37] M. Mahlobo, P. Mjwana, M. Tladi, B. Obadele, P. Olubambi, and P. Refait, "Evaluation of cathodic protection performance of carbon steel pipeline buried in soil: A review," in *2018 IEEE 9th International Conference on Mechanical and Intelligent Manufacturing Technologies (ICMIMT)*, (2018), pp. 37-43.

[38] S. Kharzi, M. Haddadi, A. Malek, L. Barazane, and M. Krishan, "Optimized design of a photovoltaic cathodic protection," *Arabian Journal for Science and Engineering,* vol. 34, p. 477, (2009).

[39] S. Goidanich, L. Lazzari, and M. Ormellese, "AC corrosion. Part 2: Parameters influencing corrosion rate," *Corrosion Science*, vol. 52, pp. 916-922, (2010).

[40] C. Gardiner and R. Melchers, "Corrosion analysis of bulk carriers, Part I: operational parameters influencing corrosion rates," *Marine Structures*, vol. 16, pp. 547-566, (2003).

[41] R. Holland, "Corrosion testing by potentiodynamic polarization in various electrolytes," *Dental Materials*, vol. 8, pp. 241-245, (1992).

[42] J. A. Harbi, F. I. Hussein, and L. A. Sabri, "Monitoring and Control on Impressed Current Cathodic Protection for Oil Pipelines," *Al-Nahrain Journal for Engineering Sciences*, vol. 20, pp. 807-814, (2017).

[43] L. R. Meyer, "Predicting corrosion on protected buried steel natural gas distribution pipelines," Massachusetts Institute of Technology, (2016).

[44] H. Liu, Y. Dai, and Y. F. Cheng, "Corrosion of underground pipelines in clay soil with varied soil layer thicknesses and aerations," *Arabian Journal of Chemistry*, vol. 13, pp. 3601-3614, (2020).

[45] M. Tan, Y. Huo, F. Mahdavi, and M. Forsyth, "Quantifying the effects of major factors affecting the effectiveness of cathodic protection of pipelines," in *C&P 2015: Proceedings of the Corrosion & Prevention 2015 Conference*, (2015), pp. 1-10.

[46] M. Jyrkama, M. Pandey, P. Angell, and D. Munson, "Estimating External Corrosion Rates for Buried Carbon Steel Piping in Different Soil Conditions," *CNL Nuclear Review*, vol. 7, pp. 85-94, (2016).

[47] T. Nagai, H. Yamanaka, A. Nishikawa, and H. Nonaka, "Influence of Anodic Current on Corrosion Protection Conditions of Buried Steel Pipeline under Cathodic Protection," in *CORROSION 2017*, (2017).

[48] T. Shabangu, P. Shrivastava, B. T. Abe, K. B. Adedeji, and P. Olubambi, "Influence of AC interference on the cathodic protection potentials of pipelines: Towards a comprehensive picture," in *2017 IEEE AFRICON*, (2017), pp. 597-602.

[49] T. Nevell and F. Walsh, "Reference electrodes," *Transactions of the IMF*, vol. 70, pp. 144-147, (1992).

[50] S. Ito, H. Hachiya, K. Baba, Y. Asano, and H. Wada, "Improvement of the silver/silver chloride reference electrode and its application to pH measurement," *Talanta,* vol. 42, pp. 1685-1690, (1995).

[51] H. Isaacs and B. Vyas, "Scanning reference electrode techniques in localized corrosion," in *Electrochemical corrosion testing*, ed: ASTM International, (1981).

[52] D. W. Whitmore, "Cathodic Corrosion Protection with Solar Panel," ed: Google Patents, (2019).

[53] M. Janowski and A. Wantuch, "ICCP cathodic protection of tanks with photovoltaic power supply," in *E3S Web of Conferences*, (2016), p. 00029.

[54] J. C. Scully, "The fundamentals of corrosion. 2," (1978).

[55] H. Y. Lee, "Corrosion of metals," (2004).

[56] S. A. Bradford, "The practical handbook of corrosion control in soils," (2000).

[57] V. Sastri, "Types of corrosion inhibitor for managing corrosion in underground pipelines," in *Underground Pipeline Corrosion*, ed: Elsevier, (2014), pp. 166-211.

[58] Z. Yang and P. Sun, "Compare of three ways of synthesis of simple Schiff base," *Molbank,* vol. 2006, p. M514, (2006).

[59] M. Shakir, A. Abbasi, M. Azam, and A. U. Khan, "Synthesis, spectroscopic studies and crystal structure of the Schiff base ligand L derived from condensation of 2-thiophenecarboxaldehyde and 3, 3′-diaminobenzidine and its complexes with Co (II), Ni (II), Cu (II), Cd (II) and Hg (II): Comparative DNA binding studies of L and its Co (II), Ni (II) and Cu (II) complexes," *Spectrochimica Acta Part A: Molecular and Biomolecular Spectroscopy,* vol. 79, pp. 1866-1875, (2011).

[60] R. Solmaz, "Investigation of the inhibition effect of 5-((E)-4-phenylbuta-1, 3-dienylideneamino)-1, 3, 4-thiadiazole-2-thiol Schiff base on mild steel corrosion in hydrochloric acid," *Corrosion Science,* vol. 52, pp. 3321-3330, (2010).

[61] J. R. Brown, *Recommended chemical soil test procedures for the North Central Region*: Missouri Agricultural Experiment Station, University of Missouri--Columbia, (1998).

[62] M. Sazali, C. Wooi, S. Arshad, T. Wong, Z. Abdul-Malek, and H. Nabipour-Afrouzi, "Study of Soil Resistivity using Wenner Four Pin Method: Case Study," in *2020 IEEE International Conference on Power and Energy (PECon)*, (2020), pp. 386-391.

[63] N. Ali and M. A. Fulazzaky, "The empirical prediction of weight change and corrosion rate of low-carbon steel," *Heliyon*, vol. 6, p. e05050, (2020).

[64] D. G. Ellis, "Cross-sectional area measurements for tendon specimens: a comparison of several methods," *Journal of biomechanics*, vol. 2, pp. 175-186, (1969).

[65] A. C. G.-o. C. o. Metals, *Standard practice for laboratory immersion corrosion testing of metals*: ASTM International, (2004).

[66] L. Khaksar and J. Shirokoff, "Effect of elemental sulfur and sulfide on the corrosion behavior of Cr-Mo low alloy steel for tubing and tubular components in oil and gas industry," *Materials*, vol. 10, p. 430, (2017).

[67] D. S. Gupta, "Corrosion behavior of 1040 carbon steel," *Corrosion*, vol. 37, pp. 611-616, (1981).

[68] L.-d. Arriba-Rodriguez, J. Villanueva-Balsera, F. Ortega-Fernandez, and F. Rodriguez-Perez, "Methods to evaluate corrosion in buried steel structures: A review," *Metals*, vol. 8, p. 334, (2018).

[69] J. Alamilla, M. Espinosa-Medina, and E. Sosa, "Modelling steel corrosion damage in soil environment," *Corrosion Science*, vol. 51, pp. 2628-2638, (2009).

[70] USGS, "Section A: National field manual for collection of water- quality data," *Book 9: Handbooks for water- resources investigations. Techniques of water- resources investigations of the United States Geological Survey*, (1999).

[71] R. Freeland, "Review of soil moisture sensing using soil electrical conductivity," *Transactions of the ASAE*, vol. 32, pp. 2190-2194, (1989).

[72] E. A. Atekwana, E. A. Atekwana, R. S. Rowe, D. D. Werkema Jr, and F. D. Legall, "The relationship of total dissolved solids measurements to bulk electrical conductivity in an aquifer contaminated with hydrocarbon," *Journal of Applied Geophysics*, vol. 56, pp. 281-294, (2004).

[73] T. Q. Ansari, J.-L. Luo, and S.-Q. Shi, "Modeling the effect of insoluble corrosion products on pitting corrosion kinetics of metals," *NPJ Materials Degradation*, vol. 3, pp. 1-12, (2019).

[74] M. A. Fulazzaky, "Measurement of biochemical oxygen demand of the leachates," *Environmental monitoring and assessment*, vol. 185, pp. 4721-4734, (2013).

[75] N. Ali, M. A. Fulazzaky, M. S. Mustapa, M. I. Ghazali, M. Ridha, and T. Sujitno, "Assessment of fatigue and corrosion fatigue behaviours of the nitrogen ion implanted CpTi," *International journal of fatigue*, vol. 61, pp. 184-190, (2014).

[76] S. Sundjono, G. Priyotomo, L. Nuraini, and S. Prifiharni, *Corrosion behavior of mild steel in seawater from northern coast of Java and southern coast of Bali, Indonesia*: Bandung Institute of Technology, (2017).

[77] J. Alcántara, B. Chico, J. Simancas, I. Díaz, and M. Morcillo, "Marine atmospheric corrosion of carbon steel: a review," *Materials*, vol. 10, p. 406, (2017).

[78] R. Foley, "Role of the chloride ion in iron corrosion," *Corrosion*, vol. 26, pp. 58-70, (1970).

[79] A. H. Seikh, "Influence of heat treatment on the corrosion of microalloyed steel in sodium chloride solution," *Journal of Chemistry*, vol. 2013, (2013).

[80] S.-J. Song and J.-G. Kim, "Influence of magnesium ions in the seawater environment on the improvement of the corrosion resistance of low-chromium-alloy steel," *Materials*, vol. 11, p. 162, (2018).

[81] M. A. Fulazzaky, N. Ali, H. Samekto, and M. I. Ghazali, "Assessment of CpTi surface properties after nitrogen ion implantation with various doses and energies," *Metallurgical and Materials Transactions A*, vol. 43, pp. 4185-4193, (2012).

[82] J. M. Triszcz, A. Porta, and F. S. G. Einschlag, "Effect of operating conditions on iron corrosion rates in zero-valent iron systems for arsenic removal," *Chemical Engineering Journal*, vol. 150, pp. 431-439, (2009).

[83] H. M. Abd El-Lateef, V. Abbasov, L. Aliyeva, E. Qasimov, and I. Ismayilov, "Inhibition of carbon steel corrosion in CO2-saturated brine using some newly surfactants based on palm oil: experimental and theoretical investigations," *Materials Chemistry and Physics*, vol. 142, pp. 502-512, (2013).

[84] V. M. Abbasov, H. M. A. El-Lateef, L. I. Aliyeva, I. T. Ismayilov, E. E. Qasimov, and M. M. Narmin, "Efficient complex surfactants from the type of fatty acids as corrosion inhibitors for mild steel C1018 in CO 2-environments," *Journal of the Korean Chemical Society*, vol. 57, pp. 25-34, (2013).

[85] E. Akbarzadeh, M. M. Ibrahim, and A. A. Rahim, "Corrosion inhibition of mild steel in near neutral solution by kraft and soda lignins extracted from oil palm empty fruit bunch," *Int. J. Electrochem. Sci*, vol. 6, pp. 5396-5416, (2011).

[86] C. Cao, "On electrochemical techniques for interface inhibitor research," *corrosion science*, vol. 38, pp. 2073-2082, (1996).

[87] F. Farelas and A. Ramirez, "Carbon dioxide corrosion inhibition of carbon steels through bis-imidazoline and imidazoline compounds studied by EIS," *Int. J. Electrochem. Sci*, vol. 5, pp. 797-814, (2010).

[88] A.-R. El-Sayed, H. S. Mohran, and H. M. Abd El-Lateef, "The inhibition effect of 2, 4, 6-tris (2-pyridyl)-1, 3, 5-triazine on corrosion of tin, indium and tin–indium alloys in hydrochloric acid solution," *Corrosion science*, vol. 52, pp. 1976-1984, (2010).

[89] D. Lopez, S. N. Simison, and S. De Sanchez, "Inhibitors performance in CO2 corrosion: EIS studies on the interaction between their molecular structure and steel microstructure," *Corrosion science*, vol. 47, pp. 735-755, (2005).

[90] L. L. Wong, S. I. Martin, and R. l. B. Rebak, "Methods to calculate corrosion rates for alloy 22 from polarization resistance experiments," in *ASME Pressure Vessels and Piping Conference*, (2006), pp. 571-580.

[91] J. Crolet, N. Thevenot, and S. Nesic, "Role of conductive corrosion products in the protectiveness of corrosion layers," *Corrosion*, vol. 54, pp. 194-203, (1998).

[92] K. Videm and J. Kvarekvål, "Corrosion of carbon steel in carbon dioxide-saturated solutions containing small amounts of hydrogen sulfide," *Corrosion*, vol. 51, pp. 260-269, (1995).

[93] R. Prabhu, T. Venkatesha, A. Shanbhag, G. Kulkarni, and R. Kalkhambkar, "Inhibition effects of some Schiff's bases on the corrosion of mild steel in hydrochloric acid solution," *Corrosion Science,* vol. 50, pp. 3356-3362, (2008).